COSMOLOGY: my "biased" (over)view

Sabino Matarrese
Dipartimento di Fisica "*Galileo Galilei*",
Università degli Studi di Padova, ITALY
email: sabino.matarrese@pd.infn.it

Planck & Planck


esa
ariane

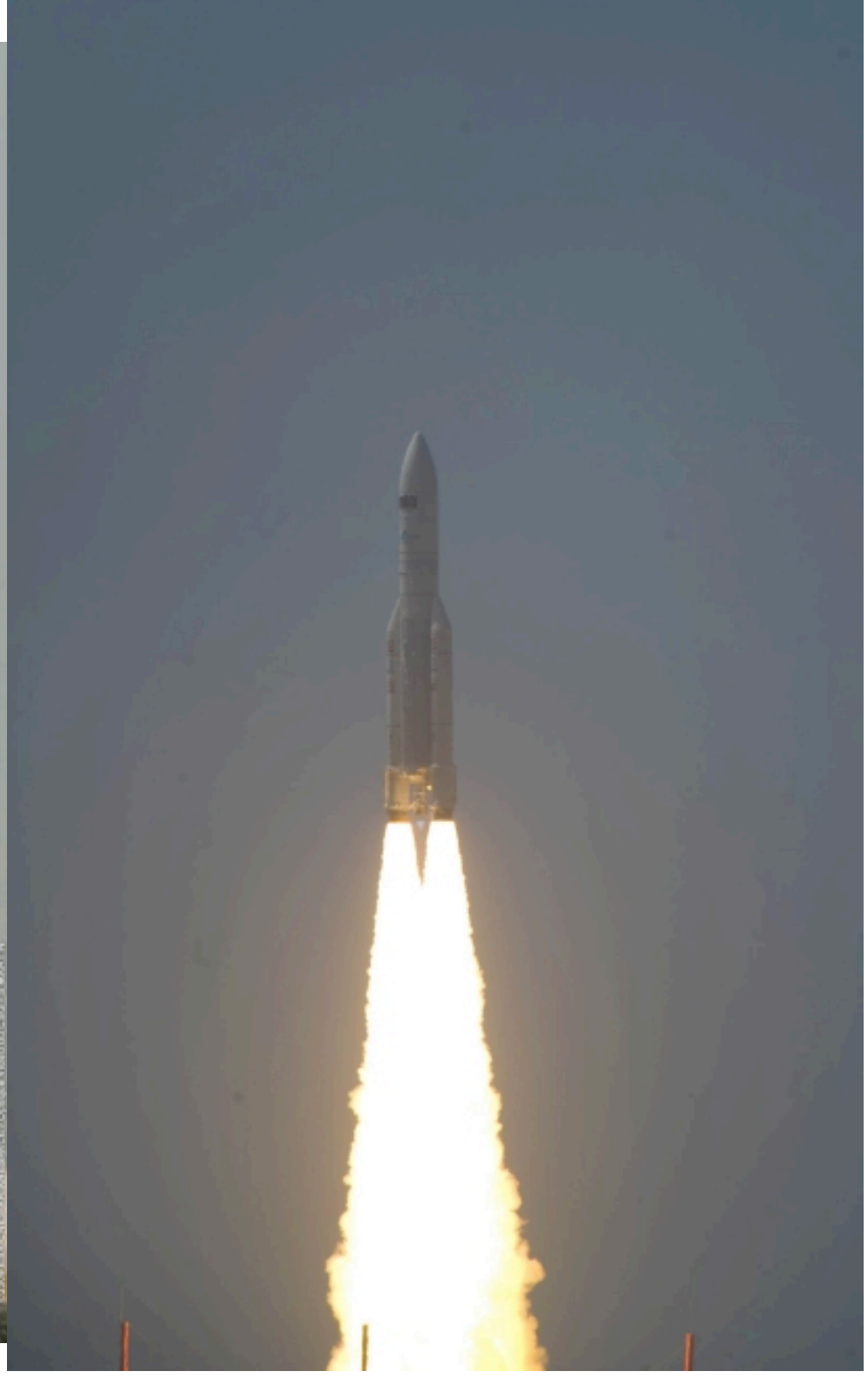

Precision Cosmology: from “what” to “why”

- “Now that key cosmological parameters have been determined to within a few percent, we anticipate a generation of experiments that move beyond adding precision to measurements of what the universe is made of, but instead help us learn **why the universe has the form we observe**. […] observational cosmology will probe the detailed dynamics of the universe in the earliest instants after the Big Bang, and start to yield clues about the physical laws that governed that epoch. Future experiments will plausibly reveal the dynamics responsible both for the large-scale homogeneity and flatness of the universe, and for the primordial seeds of small-scale inhomogeneities, including our own galaxy.” (Baumann et al. 2008, *CMBpol mission concept study*)

Label	Definition	Physical Origin	Value
Ω_b	Baryon Fraction	Baryogenesis	0.0456 ± 0.0015
$\Omega_{\rm CDM}$	Dark Matter Fraction	TeV-Scale Physics (?)	0.228 ± 0.013
Ω_Λ	Cosmological Constant	Unknown	0.726 ± 0.015
τ	Optical Depth	First Stars	0.084 ± 0.016
h	Hubble Parameter	Cosmological Epoch	0.705 ± 0.013
A_s	Scalar Amplitude	Inflation	$(2.445 \pm 0.096) \times 10^{-9}$
n_s	Scalar Index	Inflation	0.960 ± 0.013

Physical Origin of Cosmological Parameters

Label	Definition	Physical Origin
Ω_k	Curvature	Initial Conditions
Σm_ν	Neutrino Mass	Beyond-SM Physics
w	Dark Energy Equation of State	Unknown
N_ν	Neutrino-like Species	Beyond-SM Physics
$Y_{\rm He}$	Helium Fraction	Nucleosynthesis
α_s	Scalar "Running"	Inflation
A_t	Tensor Amplitude	Inflation
n_t	Tensor Index	Inflation
$f_{\rm NL}$	Non-Gaussianity	Inflation (?)
S	Isocurvature	Inflation
$G\mu$	Topological Defects	Phase Transition

CMB: a Window to the Physics of the Early Universe

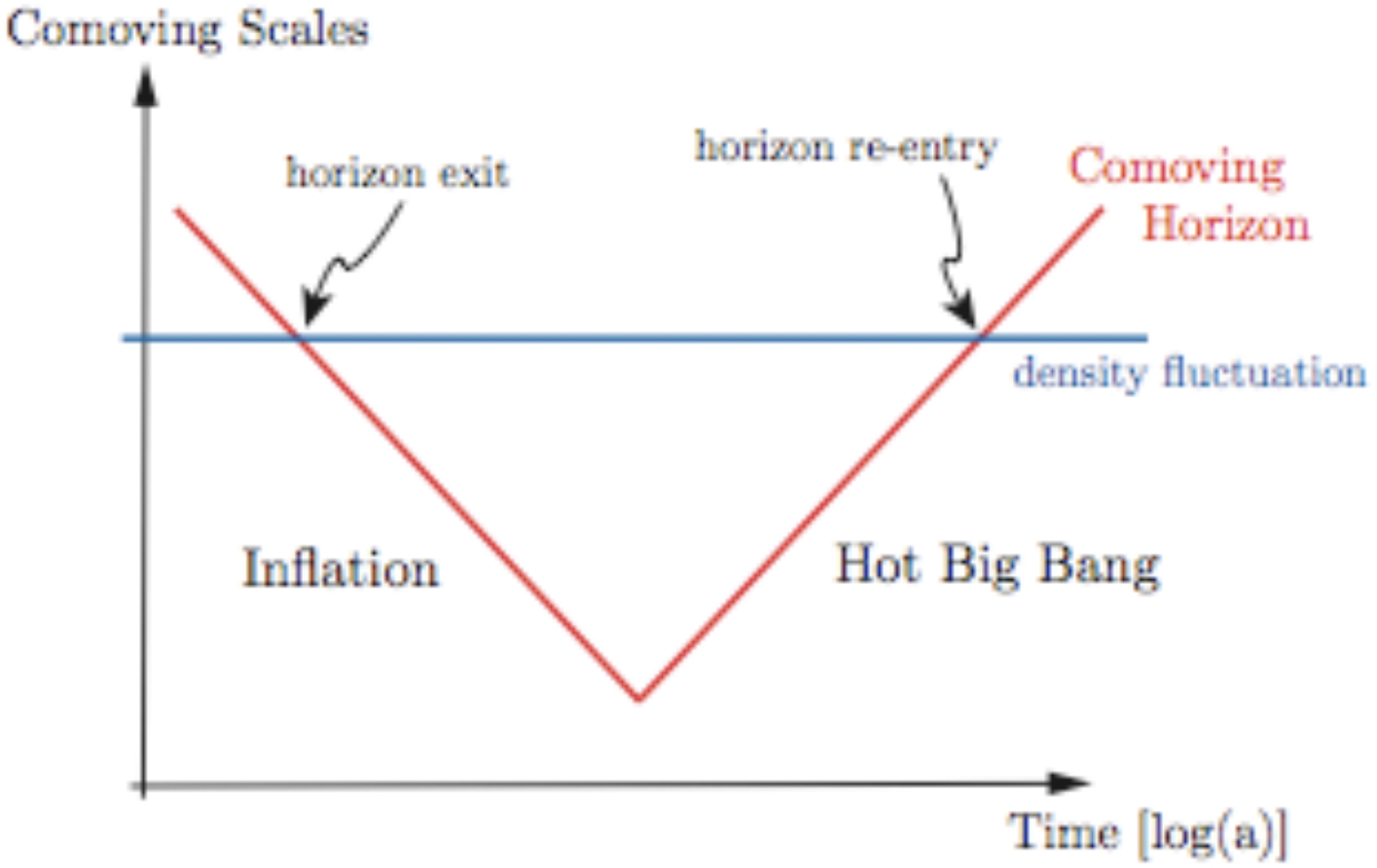

Inflation and Observational Cosmology: where do we stand?

Label	Definition	Physical Origin	Current Status
A_s	Scalar Amplitude	V, V'	$(2.445 \pm 0.096) \times 10^{-9}$
n_s	Scalar Index	V', V''	0.960 ± 0.013
α_s	Scalar Running	V', V'', V'''	only upper limits
A_t	Tensor Amplitude	V (Energy Scale)	only upper limits
n_t	Tensor Index	V'	only upper limits
r	Tensor-to-Scalar Ratio	V'	only upper limits
Ω_k	Curvature	Initial Conditions	only upper limits
$f_{\rm NL}$	Non-Gaussianity	Non-Slow-Roll, Multi-Field	only upper limits
S	Isocurvature	Multi-Field	only upper limits
$G\mu$	Topological Defects	End of Inflation	only upper limits

The determination of most of these parameters requires the combination of LSS and CMB data on both large and small scales.

Testable predictions of inflation

- ✓ Cosmological aspects
  - Critical density Universe
  - Almost scale-invariant and nearly Gaussian, adiabatic density fluctuations
  - Almost scale-invariant stochastic background of relic gravitational waves
- ✓ Particle physics aspects
  - Nature of the inflaton
  - Inflation energy scale

Sources of GWs

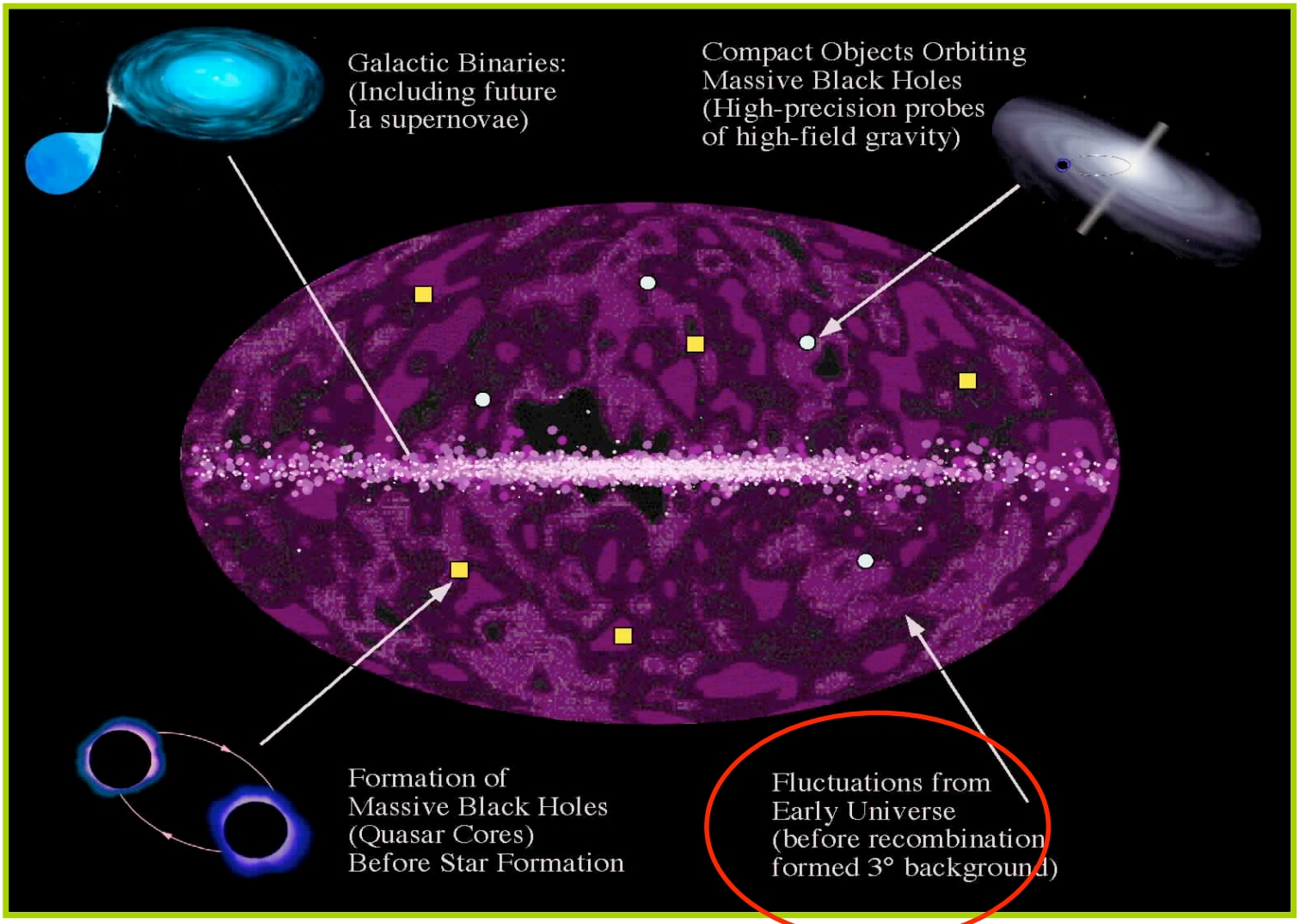

THE GRAVITATIONAL WAVE SPECTRUM

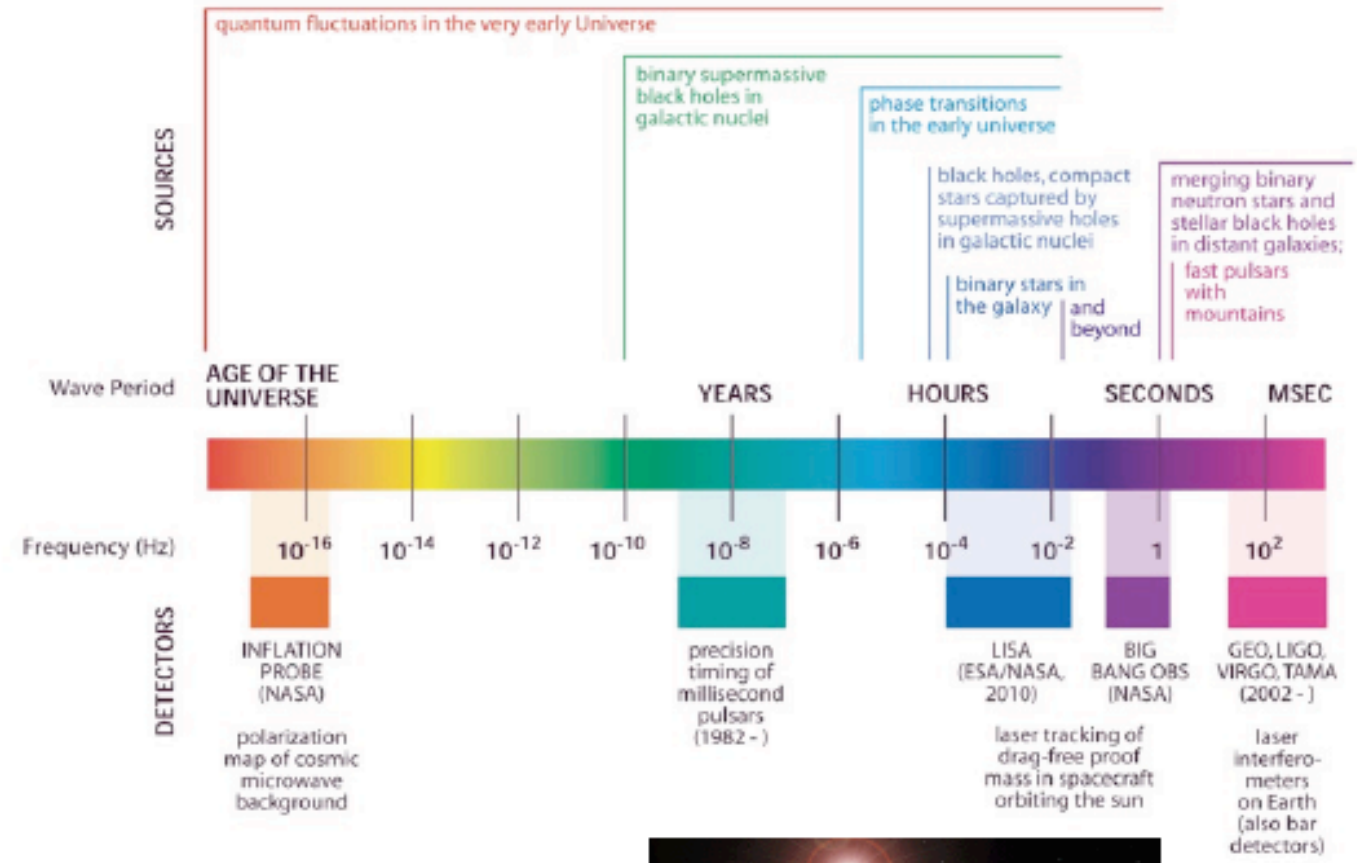

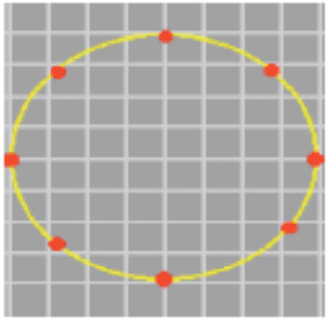

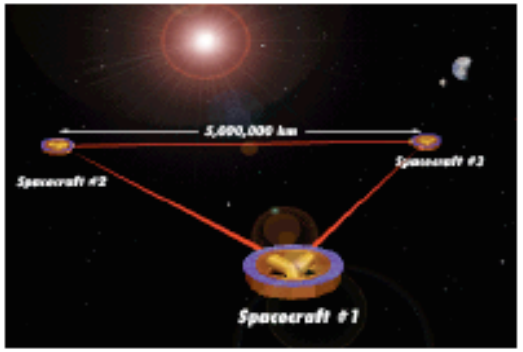

LISA (~2012;
test flight next year)

Gravity waves: the “smoking gun” of inflation

- ✓ The spectra $P_R(k)$ and $P_T(k)$ provide the contact between theory and observations. The *WMAP* (+SDSS) dataset allows to extract an upper bound, $r<0.28$ (95% CL) (Spergel 2006), or $\varepsilon<0.017$. This limit provides un upper bound on the energy scale of inflation

$$V^{1/4} < 2.6 \times 10^{16} \text{ GeV}$$

- ✓ A positive detection of the B-mode in CMB polarization, and therefore an indirect evidence of gravitational waves from inflation, once foregrounds due to gravitational lensing from local sources has been properly treated, requires $\varepsilon > 10^{-5}$, corresponding to

$$V^{1/4} > 3.5 \times 10^{15} \text{ GeV}$$

Probing Inflation with CMB Polarization

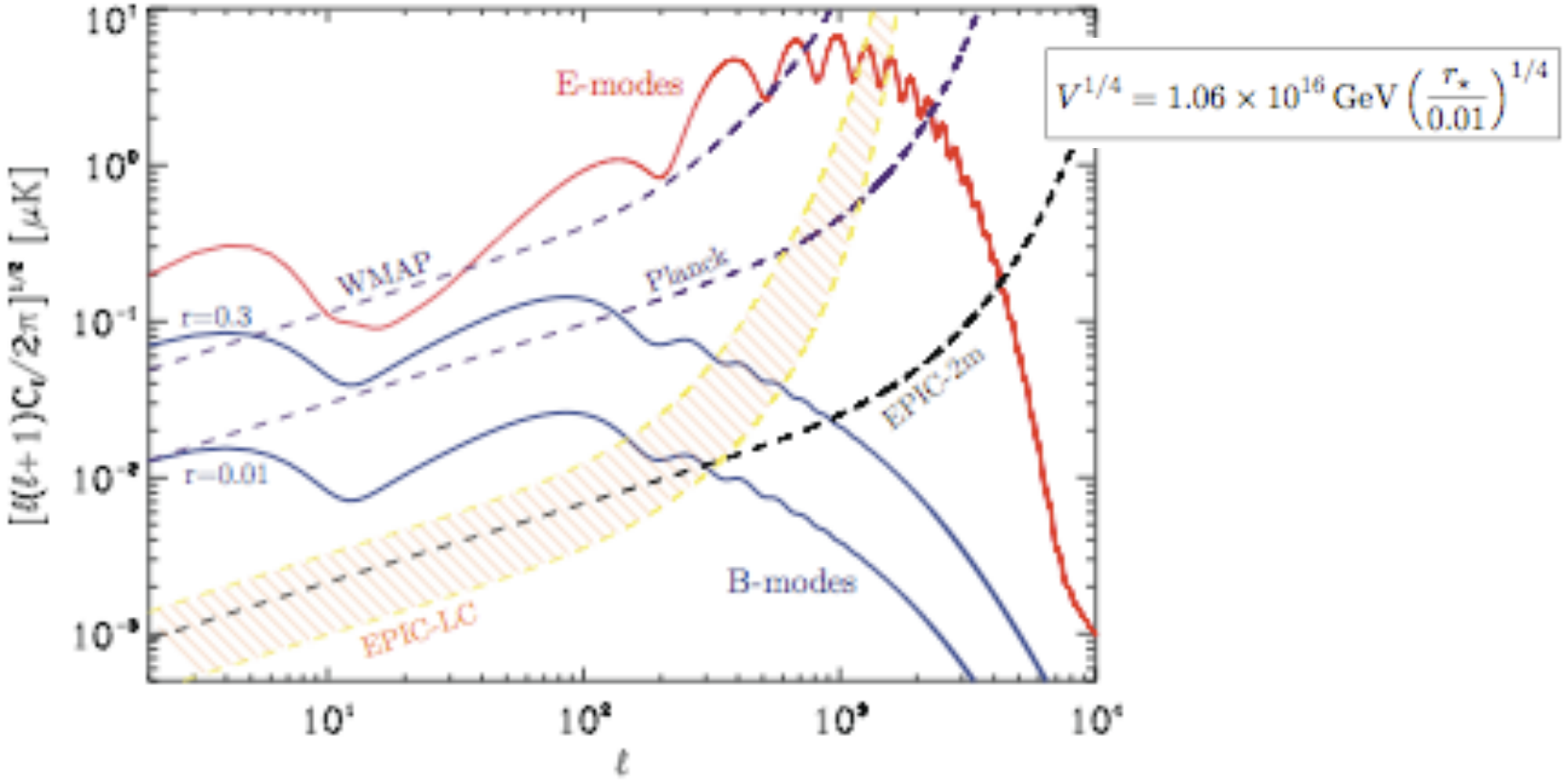

E- and B-mode power spectra for a tensor-to-scalar ratio saturating current bounds, $r = 0.3$, and for $r = 0.01$. Shown are also the experimental sensitivities for *WMAP*, *Planck* and two different realizations of *CMBPol* (EPIC-LC and EPIC-2m). (Figure adapted from Bock *et al.* [59].)

Tensor-to-scalar ratio

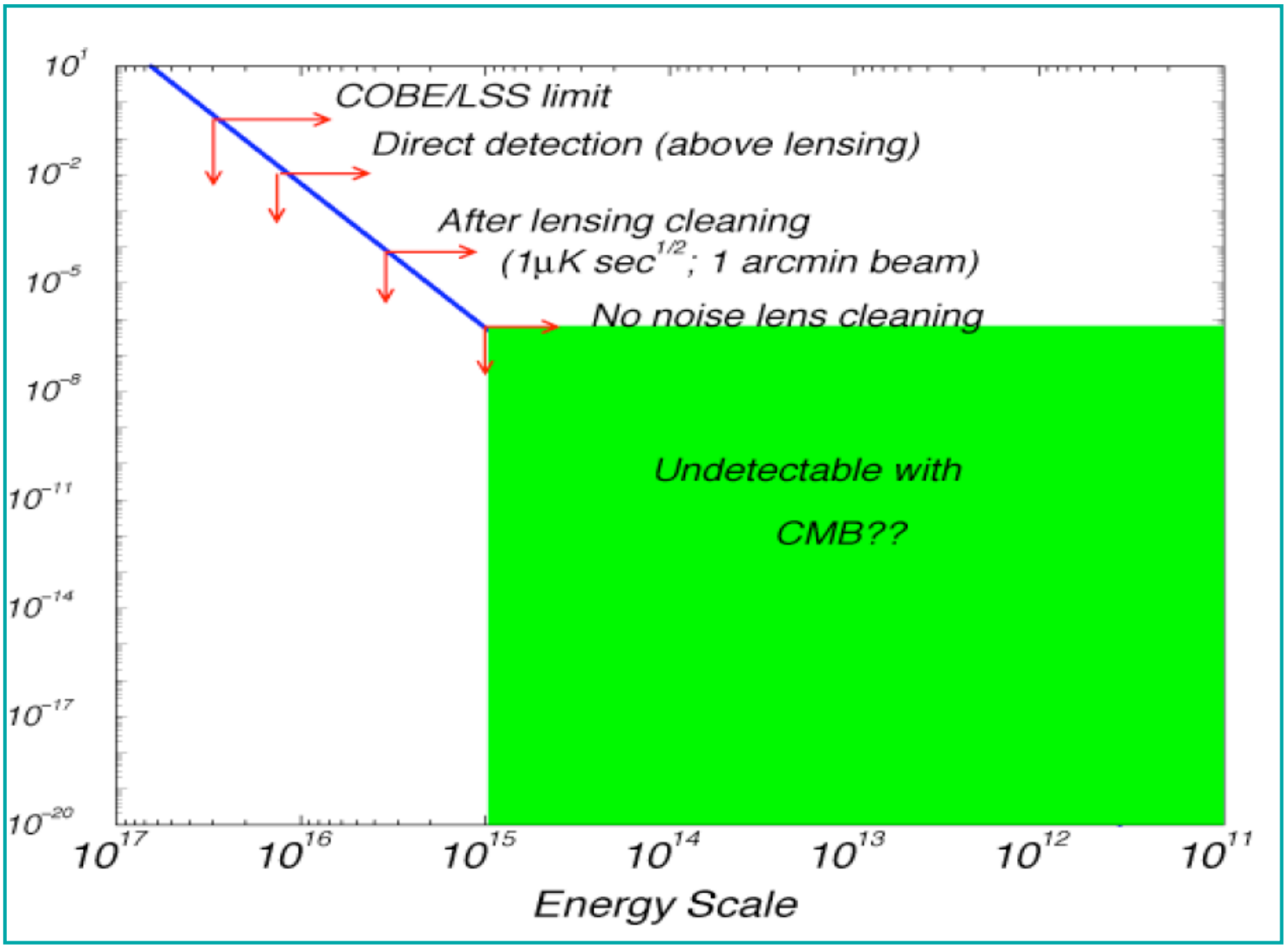

Cooray 2004

Second-order tensor modes

Second-order metric

$$ds^2 = a^2(\eta)[-(1 + 2\Phi^{(1)} + 2\Phi^{(2)})d\eta^2 + 2V_i^{(2)}d\eta dx^i + \{(1 - 2\Psi^{(1)} - 2\Psi^{(2)})\delta_{ij} + \tfrac{1}{2}h_{ij}\}dx^i dx^j],$$

Second-order tensor modes

$$h_{ij}'' + 2\mathcal{H}h_{ij}' - \nabla^2 h_{ij} = -4\hat{\mathcal{T}}_{ij}^{\ lm}\mathcal{S}_{lm}$$

tensor projector

$$\begin{aligned}\mathcal{S}_{ij} \equiv\ & 2\Phi\partial^i\partial_j\Phi - 2\Psi\partial^i\partial_j\Phi + 4\Psi\partial^i\partial_j\Psi + \partial^i\Phi\partial_j\Phi \\ & - \partial^i\Phi\partial_j\Psi - \partial^i\Psi\partial_j\Phi + 3\partial^i\Psi\partial_j\Psi \\ & - \frac{4}{3(1+w)\mathcal{H}^2}\partial_i(\Psi' + \mathcal{H}\Phi)\partial_j(\Psi' + \mathcal{H}\Phi) \\ & - \frac{2c_s^2}{3w\mathcal{H}^2}[3\mathcal{H}(\mathcal{H}\Phi - \Psi') + \nabla^2\Psi]\partial_i\partial_j(\Phi - \Psi).\end{aligned}$$

GW from non-linear cosmological perturbations

tensor-mode projection operator

$$h^{\alpha}{}_{\beta}(\eta,\mathbf{x}) = \frac{4G}{c^4}\frac{1}{ar}\mathcal{P}^{\alpha}{}_{\nu}{}^{\mu}{}_{\beta}\left[a^3\int d^3\tilde{x}\,\mathcal{R}^{\nu}_{\mathrm{eff}\,\mu}\right]_{ret}$$

$$\mathcal{R}^{\alpha}_{\mathrm{eff}\,\beta} = \rho\left(v^{\alpha}v_{\beta} - \frac{1}{3}v^2\,\delta^{\alpha}{}_{\beta}\right) + \\ + \frac{1}{4\pi G a^2}\left(\partial^{\alpha}\varphi\,\partial_{\beta}\varphi - \frac{1}{3}\partial^{\nu}\varphi\,\partial_{\nu}\varphi\,\delta^{\alpha}{}_{\beta}\right)$$

Carbone & Matarrese 2005

Tensor (and vector!) metric modes are generated by scalar (e.g. density) perturbations as soon as the latter become non-linear. As a result GW are produced during the later stages of cosmological structure formation with typical period of the order of the Hubble time.

Secondary tensors

Matarrese, Mollerach & Bruni 1998; Mollerach, Harari & Matarrese 2004; Ananda, Clarkson & Wands 2007; Baumann, Steinhardt, Takahashi & Ichiki 2007, Mangilli, Bartolo, Matarrese & Riotto (2008) computed the GW background produced at second-order by scalar modes in various epochs. According to Baumann et al. these second-order modes may even dominate the primary background on intermediate scales. For cyclic/ekpyrotic models they always dominate.

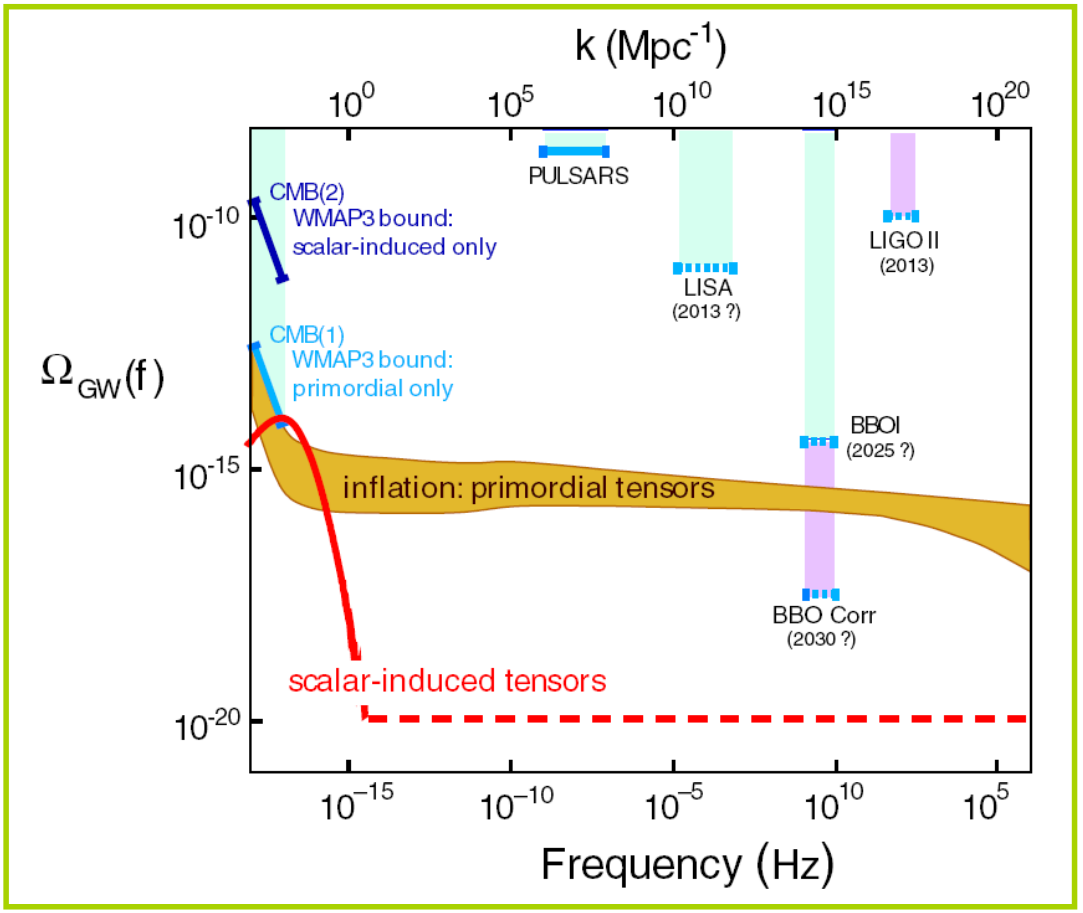

Baumann et al. 2007

Curvaton and GWs

In the curvaton scenario for the generation of perturbation, the production of primary tensor modes is suppressed by the requirement that inflaton Perturbations have negligible amplitude. Bartolo, Matarrese, Riotto & Väihkönen (2007) have shown that second-order tensor modes can have a non-negligible amplitude, being proportional to the non-Gaussianity strength f_{NL}

For $f_{NL} \sim 100$ one can easily attain values as large as $\Omega_{GW} \sim 10^{-15}$ in the frequency range relevant for BBO or DECIGO

CMB weak-gravitational lensing: a foreground for the (indirect) detection of primordial gravitational waves via B-mode polarization

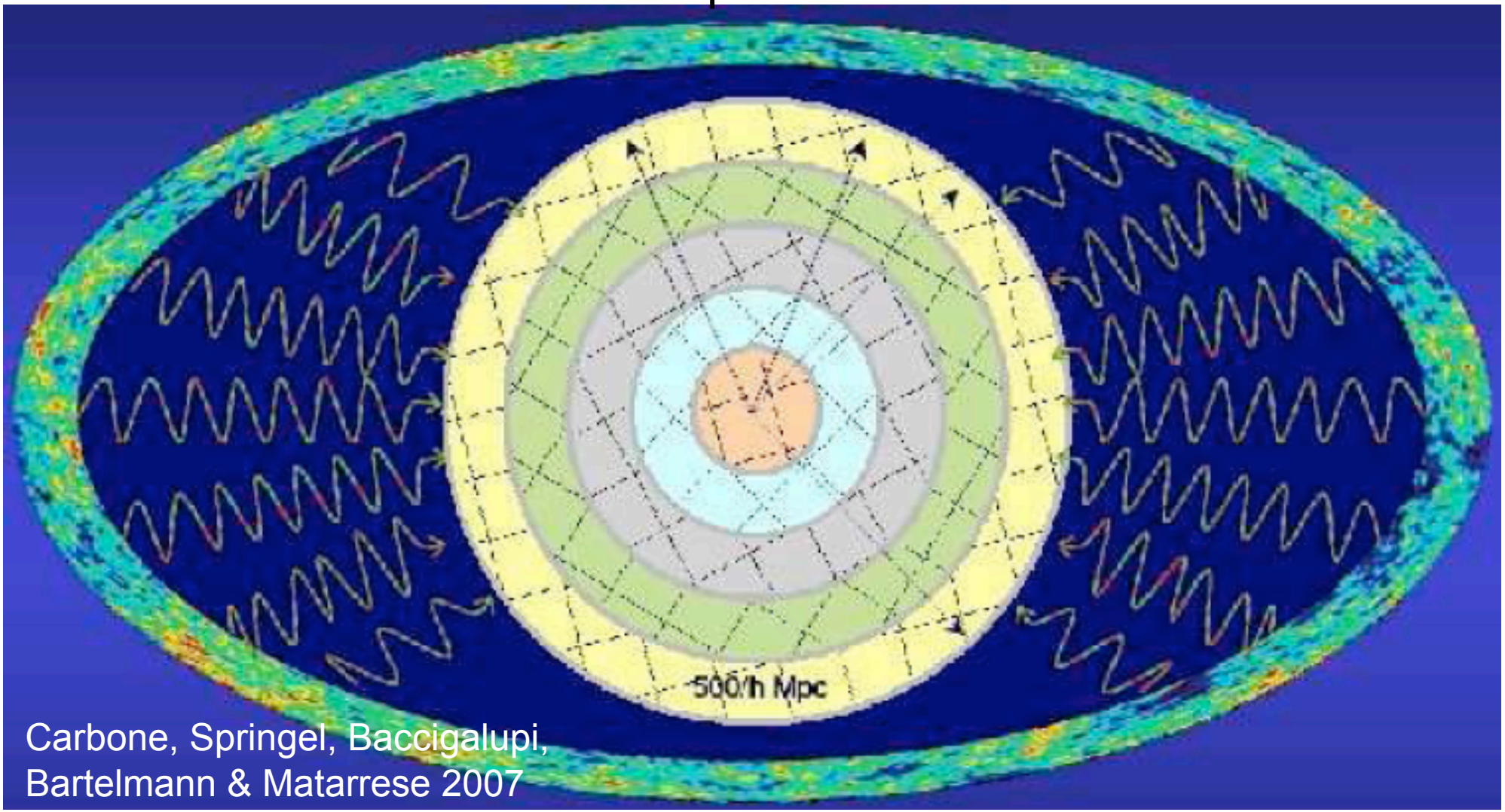

Figure 1. Sketch of the adopted stacking and randomization process. The passage of CMB photons through the dark matter distribution of the Universe is followed by stacking the gravitational potential boxes of the MS, which are $500\,h^{-1}$Mpc on a side (comoving). Shells of thickness $500\,h^{-1}$Mpc are filled with periodic replicas of the box. All boxes (squares) that fall into the same shell are randomized with the same coordinate transformation (rotation and translation), which, in turn, differs from shell to shell.

Lensed CMB

- Map of the polarization induced by LSS on the CMB obtained from the Millennium simulation (Carbone, Baccigalupi, Bartelmann, Matarrese & Springel 2008)

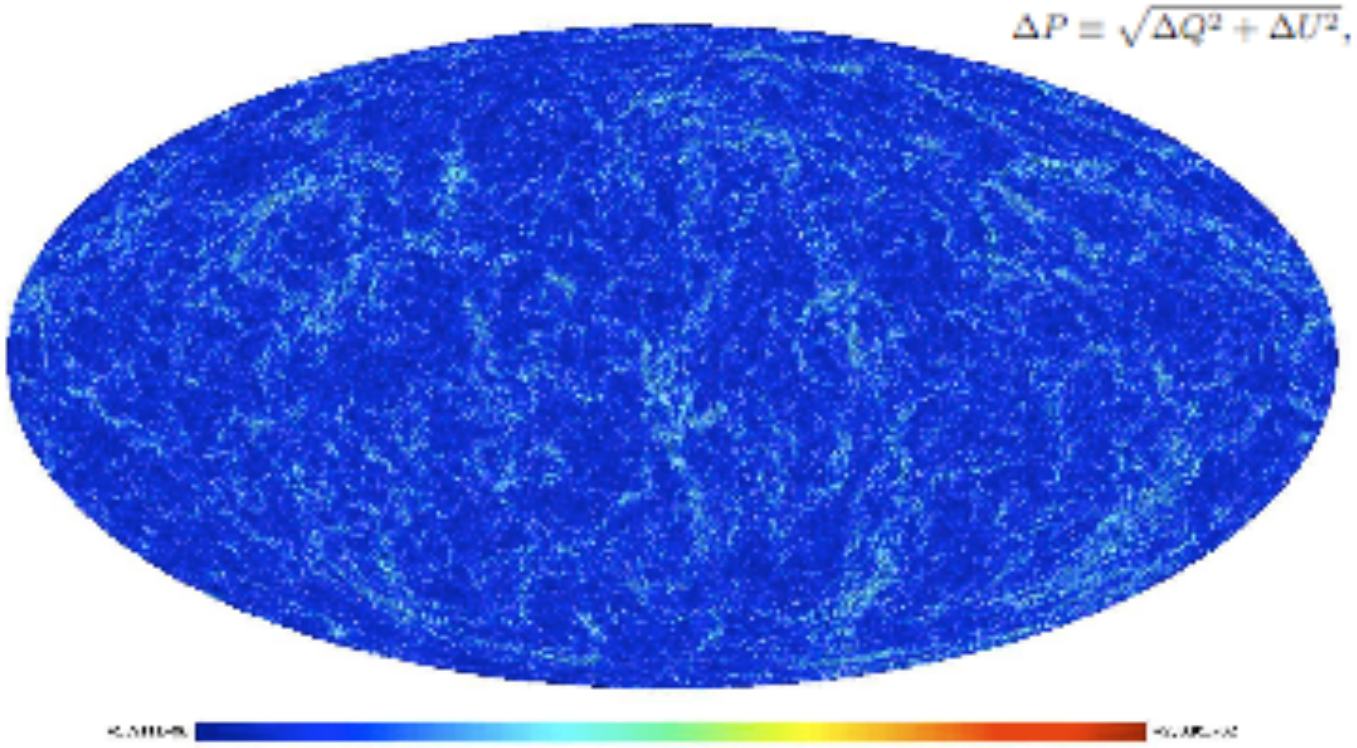

Non-Gaussianity

- Alternative structure formation models of the late eighties considered strongly non-Gaussian primordial fluctuations.
- The increased accuracy in CMB and LSS observations has excluded this extreme possibility.
- The present-day challenge is either detect or constrain mild or weak (~0.1%) deviations from primordial Gaussian initial conditions.
- Deviations of this type are not only possible but are generically predicted in the standard perturbation generating mechanism provided by inflation.

Simple-minded NG model

- ✓ Many primordial (inflationary) models of non-Gaussianity can be represented in configuration space by the simple formula (Salopek & Bond 1990; Gangui et al. 1994; Verde et al. 1999; Komatsu & Spergel 2001)

$$\Phi = \phi_L + f_{NL} * (\phi_L^2 - \langle \phi_L^2 \rangle) + g_{NL} * \phi_L^3 + \ldots$$

where Φ is the large-scale gravitational potential, ϕ_L its linear Gaussian contribution and f_{NL} is the dimensionless *non-linearity parameter* (or more generally *non-linearity function*). The percent of non-Gaussianity in CMB data implied by this model is

$$\text{NG \%} \sim 10^{-5} |f_{NL}|$$

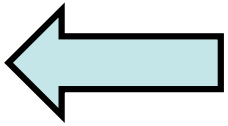

$< 10^{-3}$ from *WMAP*

Inflationary predictions for f_{NL}

Models	$f_{\rm NL}$	Comments
Single–field inflation	$\mathcal{O}(\epsilon,\eta)$	ϵ,η slow-roll parameters
Curvaton scenario	$\frac{5}{4r}-\frac{5}{6}r-\frac{5}{3}$	$r\approx\left(\frac{\rho_\sigma}{\rho}\right)_{decay}$
Inhomogeneous reheating	$-\frac{5}{4}-I$	$I=-\frac{5}{2}+\frac{5}{12}\frac{\Gamma}{\alpha\Gamma_1}$ "minimal case" $I=0$ $(\alpha=\frac{1}{6},\,\Gamma_1=\bar{\Gamma})$
Multiple scalar fields	$\frac{\mathcal{P}_\mathcal{S}}{\mathcal{P}_\mathcal{R}}\cos^2\Delta\left(4\cdot10^3\cdot\frac{V_{\chi\chi}}{3H^2}\right)\cdot60\frac{H}{\chi}$	order of magnitude estimate of the absolute value
Warm inflation	$-\frac{5}{6}\left(\frac{\dot{\varphi}_0}{H^2}\right)\left[\ln\left(\frac{\Gamma}{H}\right)\frac{V'''}{\Gamma}\right]$	Γ: inflaton decay rate
Ghost inflation	$-85\cdot\beta\cdot\alpha^{-8/5}$	equilateral configuration
DBI	$-0.2\,\gamma^2$	equilateral configuration
Preheating scenarios	e.g. $\frac{M_{Pl}}{\varphi_0}e^{Nq/2}\sim50$	N: number of inflaton oscillations
Inhomogeneous preheating and inhomogeneous hybrid inflation	e.g. $\frac{5}{6}\lambda_\varphi\left(\frac{M_{Pl}}{m_\chi}\right)^2\sim100$	λ_φ: inflaton coupling to the waterfall field χ
Generalized single-field inflation (including k-inflation and brane inflation)	$-\frac{35}{108}\left(\frac{1}{c_s^2}-1\right)+\frac{5}{81}\left(\frac{1}{c_s^2}-1-2\frac{\lambda}{\Sigma}\right)$	high when the sound speed $c_s\ll1$ or $\lambda/\Sigma\gg1$

Inflationary predictions for f_{NL}

Table 1.2 Predictions for $f_{\rm NL}$ from some unconventional scenarios

Models	$f_{\rm NL}$	Comments
Warm inflation	$-15L(r) < f_{\rm NL} < (33/2)L(r)$	$L(r) \simeq \ln(1 + r/14)$; $r = \frac{\Gamma}{3H} \gg 1$
Generalized slow-roll/ higher-order kin. terms	$f_{\rm NL} \gg +1$	equilateral config.
Excited in. states + interact.	$\sim \left(6.3 \times 10^{-4} \frac{M_P}{M}\right)^5 \sim (1 - 100)$	flatten config. M: cut-off scale
Ekpyrotic models	$-50 \leq f_{\rm NL} \leq +200$	depends on sharpness of conversion from isocurv. to curvature modes.

NG (and anisotropy) from non-Abelian vector modes

- Bartolo, Dimastrogiovanni, Matarrese & Riotto, in prep.

  – *Non-Gaussianity.* Primordial vector fields might generate a larger non-Gaussianity than the one observed in standard inflation.

  – *Anisotropy.* Violation of primordial rotational invariance from vector fields introduces some degree of anisotropy in the correlation functions.

  We generalize the Abelian case (Dimopoulos et al, arXiv:0809.1055), considering an $SU(2)$ gauge multiplet non-minimally coupled to gravity during inflation

$$S = \int d^4x\sqrt{-g}\Big[\frac{m_p^2 R}{2} - \frac{1}{4}g^{\mu\alpha}g^{\nu\beta}F^a_{\mu\nu}F^a_{\alpha\beta} - \frac{1}{2}\left(m^2 + \xi R\right)g^{\mu\nu}B^a_\mu B^a_\nu + L_\phi\Big],$$

- Possible realizations: vector curvaton / vector inflation

- NG can be large → **see E. Dimastrogiovanni's poster**

NG CMB simulated maps

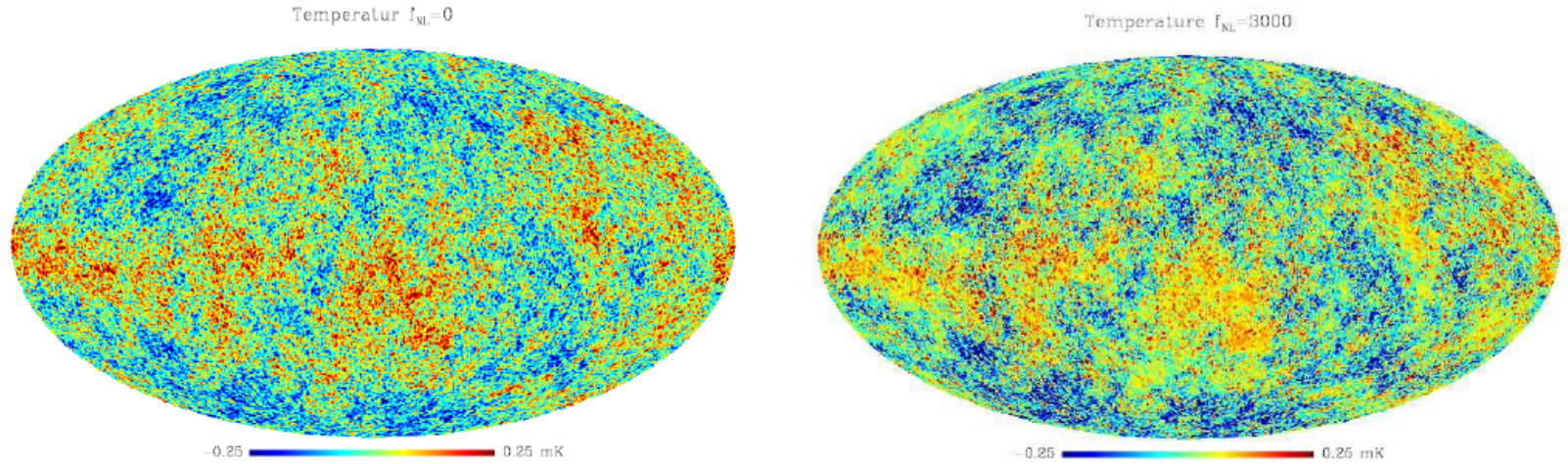

Liguori, Yadav, Hansen, Komatsu, Matarrese & Wandelt 2007

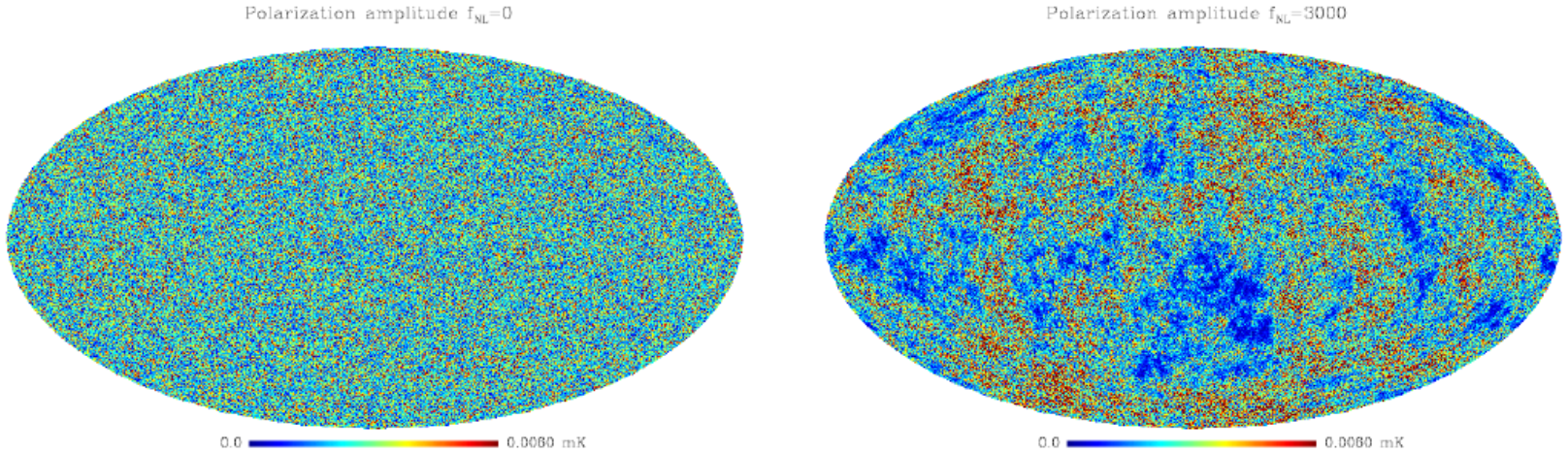

FIG. 8: Left column: temperature and polarization intensity Gaussian CMB simulations obtained from our algorithm. Polarization intensity is defined as $I \equiv \sqrt{Q^2 + U^2}$ where Q and U are the Stokes parameters. Right column: temperature and polarization non-Gaussian maps with the same Gaussian seed as in the left column and $f_{\rm NL} = 3000$. The reason for the choice of such a large $f_{\rm NL}$ is that we wanted to make non-Gaussian effects visible by eye in the figures. The cosmological model adopted for this plots is characterized by: $\Omega_b = 0.042$, $\Omega_{cdm} = 0.239$, $\Omega_L = 0.719$, $h = 0.73$, $n = 1$, $\tau = 0.09$. Temperatures are in mK.

Summary of NG from inflation

Bartolo, Matarrese & Riotto 2005; Boubeker, Creminelli, D'Amico, Noreña & Vernizzi 2009

$$\delta T/T = -(\Phi/3)$$

$$\Phi = \Phi_{\rm L} + f_{\rm NL} \star (\Phi_{\rm L})^2 + g_{\rm NL} \star (\Phi_{\rm L})^3,$$

leading contribution to bispectrum:

- Quadratic non-linearity on large-scales (up to ISW and 2-nd order tensor modes). Standard slow-roll inflation yields $a_{NL} \sim b_{NL} \sim 1$

Include SW + ISW up to 3-rd order

$$f_{\rm NL} = -\left[\tfrac{5}{3}(1-a_{\rm NL}) + \tfrac{1}{6}\right] + \left[3(\mathbf{k}_1\cdot\mathbf{k}_3)(\mathbf{k}_2\cdot\mathbf{k}_3)/k^4 - (\mathbf{k}_1\cdot\mathbf{k}_2)/k^2\right] \quad \text{- } \cos(2\vartheta)$$

additional contribution to trispectrum (together with f_{NL}^2 terms):

- Cubic non-linearity on large-scales (up to ISW and 2-nd order tensor modes)

$$g_{\rm NL}(\mathbf{k}_1,\mathbf{k}_2,\mathbf{k}_3) = \tfrac{25}{9}(b_{\rm NL}-1) + \tfrac{25}{9}(a_{\rm NL}-1)\mathcal{A}(\mathbf{k}_1,\mathbf{k}_2,\mathbf{k}_3) + \tfrac{25}{9}\mathcal{C}(\mathbf{k}_1,\mathbf{k}_2,\mathbf{k}_3) - \tfrac{5}{9}(a_{\rm NL}-1)$$
$$+ \frac{1}{54} - \frac{1}{3}\left[\frac{(\mathbf{k}_1\cdot(\mathbf{k}_1+\mathbf{k}_2))\,(\mathbf{k}_2\cdot(\mathbf{k}_1+\mathbf{k}_2))}{|\mathbf{k}_1+\mathbf{k}_2|^4} - \frac{1}{3}\frac{\mathbf{k}_1\cdot\mathbf{k}_2}{|\mathbf{k}_1+\mathbf{k}_2|^2} + \text{cycl.}\right],$$

The shape of Non-Gaussianities

Different models for the generation of NG may lead to a different shape dependence of the bispectrum, which is very important for constraining NG

squeezed configurations dominant

equilateral configurations approximately dominant

Babich et al. 2005; Creminelli et al. 2005; LoVerde et al. 2007

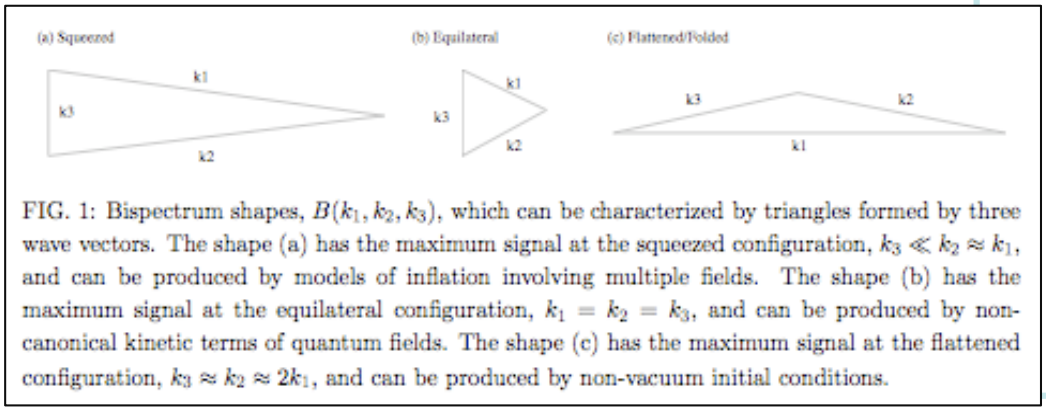

FIG. 1: Bispectrum shapes, $B(k_1, k_2, k_3)$, which can be characterized by triangles formed by three wave vectors. The shape (a) has the maximum signal at the squeezed configuration, $k_3 \ll k_2 \approx k_1$, and can be produced by models of inflation involving multiple fields. The shape (b) has the maximum signal at the equilateral configuration, $k_1 = k_2 = k_3$, and can be produced by non-canonical kinetic terms of quantum fields. The shape (c) has the maximum signal at the flattened configuration, $k_3 \approx k_2 \approx 2k_1$, and can be produced by non-vacuum initial conditions.

local

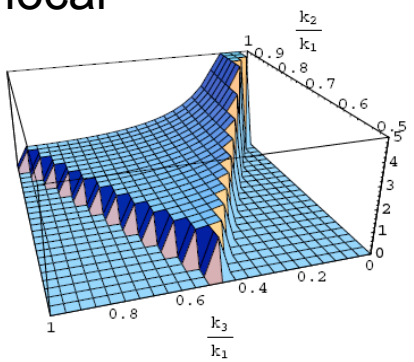

(a)

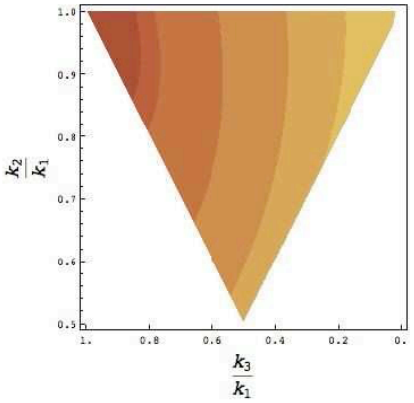

(b)

DBI

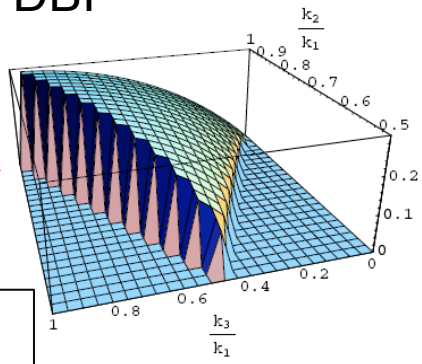

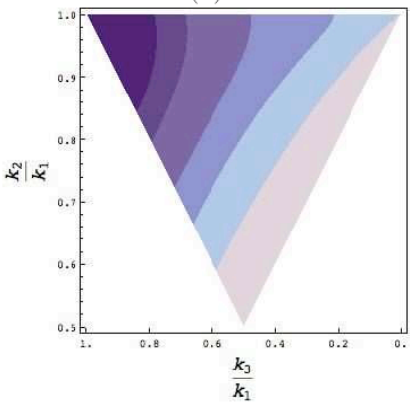

LoVerde et al. 2007

Figure 2: (a) The shape of the primordial bispectrum for the local model, $\mathcal{A}_{local}(1, k_2, k_3)/(k_2 k_3)/f_{NL}$. The domain of the plot is restricted to $\mathbf{k}_1 + \mathbf{k}_2 + \mathbf{k}_3 = 0$. (b) Contour plot of the fractional difference between the local form of non-Gaussianity and the DBI shape. Shaded regions show contours of (beginning from the upper left-hand corner) $(\mathcal{A}_{local} - \mathcal{A}_c)/\mathcal{A}_c$ =0, 0.05, 0.1, 0.5, 1, 2, 10. (c) The dominant shape in the primordial bispectrum for the DBI model, plotted is $\mathcal{A}_c(1, k_2, k_3)/(k_2 k_3)/f^c_{NL}$.(d) Contour plot of the fractional difference between the equilateral form of non-Gaussianity and the DBI shape. Shaded regions show contours of (beginning from the upper left-hand corner) $(\mathcal{A}_{equil} - \mathcal{A}_c)/\mathcal{A}_c = 0, 0.01, 0.02, 0.05, 0.1, 0.25$.

NG as a Test on the Physics of the Early Universe

- The bispectrum shape measures deviations from standard inflation, perturbation generating processes after inflation, initial state before inflation, super-Planckian phsyics (together with GW and running spectral index). Going to smaller scales and exploiting E-mode polarization allows to reach very high sensitivity (small f_{NL}). The limitations which apply to local NG do not necessarily apply to non-local NG (DBI inflation, Ghost, multi-field, curvaton, modulated reheating, non-Bunch-Davies initial states, …).

- Statistics of E and B modes, sensitive to CMB lensed by LSS, hence allowing to improve limits on primordial (GW induced) B modes. Non-Gaussian GW background (from pre-heating after inflation, curvaton mechanism, phase transitions, secondary GW background).

WMAP 5-years constraints on f_{NL}

Komatsu et al. (2008) find

$$-9 < f_{NL}^{\rm local} < 111 \ (95\% \ {\rm CL})$$

(after point-source subtraction) analyzing 5-year WMAP data.

The discrepancy with Yadav & Wandelt (2007) who found positive NG detection in 3-year WMAP data

$$27 < f_{\rm NL} < 147 \ {\rm at} \ 95\% \ {\rm C.L.}$$

(rejection of f_{NL}=0 at more than 99.5% CL) can be explained in terms of the different mask applied in the analysis.

Smith et al. (2009) have used the optimal estimator for local NG to find

$$-4 < f_{\rm NL} < 80 \ {\rm at} \ 95\% \ {\rm C.L.}$$

TABLE 5
CLEAN-MAP ESTIMATES AND THE CORRESPONDING 68% INTERVALS OF THE LOCAL FORM OF PRIMORDIAL NON-GAUSSIANITY, $f_{NL}^{\rm local}$, THE POINT SOURCE BISPECTRUM AMPLITUDE, b_{src} (IN UNITS OF 10^{-5} $\mu{\rm K}^3$ ${\rm sr}^2$), AND MONTE-CARLO ESTIMATES OF BIAS DUE TO POINT SOURCES, $\Delta f_{NL}^{\rm local}$

Band	Mask	$l_{\rm max}$	$f_{NL}^{\rm local}$	$\Delta f_{NL}^{\rm local}$	b_{src}
V+W	*KQ85*	400	50 ± 29	1 ± 2	0.26 ± 1.5
V+W	*KQ85*	500	61 ± 26	2.5 ± 1.5	0.05 ± 0.50
V+W	*KQ85*	600	68 ± 31	3 ± 2	0.53 ± 0.28
V+W	*KQ85*	700	67 ± 31	3.5 ± 2	0.34 ± 0.20
V+W	*Kp0*	500	61 ± 26	2.5 ± 1.5	
V+W	*KQ75p1*[a]	500	53 ± 28	4 ± 2	
V+W	*KQ75*	400	47 ± 32	3 ± 2	-0.50 ± 1.7
V+W	*KQ75*	500	55 ± 30	4 ± 2	0.15 ± 0.51
V+W	*KQ75*	600	61 ± 36	4 ± 2	0.53 ± 0.30
V+W	*KQ75*	700	58 ± 36	5 ± 2	0.38 ± 0.21

[a]This mask replaces the point-source mask in *KQ75* with the one that does not mask the sources identified in the *WMAP* K-band data

Komatsu et al. 2008

Constraints on non-local NG are much weaker:

$$-151 < f_{NL}^{\rm equil} < 253 \ (95\% \ {\rm CL})$$

Constraining Non-Gaussianity from Inflation with Planck vs. ideal experiment

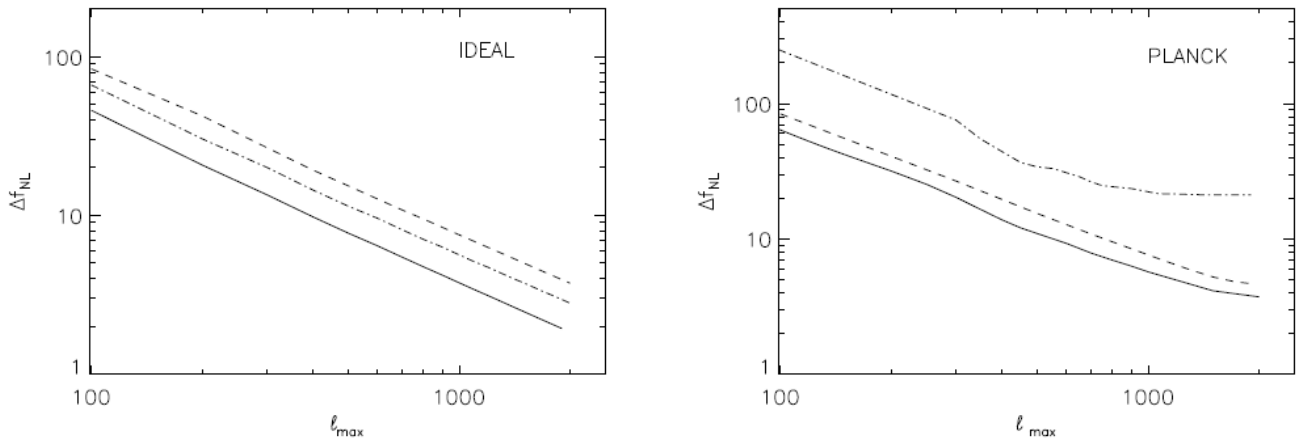

Fig. 2.— Fisher predictions for minimum detectable f_{NL} at the 1-σ level. Left panel: ideal experiment. Right panel: Planck satellite. Solid lines: temperature and polarization information combined. Dashed lines: temperature information only. Dot-dashed line: polarization information only.

Yadav, Komatsu and Wandelt 2007

Searching for NG in Planck data will require accurate handling of residual NG from systematics (foreground, point sources, NG induced by map making).

Fast estimator extended to incomplete sky coverage in Yadav, Komatsu, Wandelt, Liguori, Hansen & Matarrese 2007: see also Creminelli, Nicolis, Senatore & Tegmark 2006; covariance weighted KSW estimator used by Senatore, Smith & Zaldarriaga 2009

Second-order (radiation) transfer function

- The non-Gaussianities measurable e.g. by Planck are originated by primordial sources as well as by secondary effects + various foreground contaminants. Secondaries + foregrounds may give rise to both a bias and a variance in the determination of e.g. fNL. All secondary contributions are included in the so-called *second-order radiation transfer function* which accounts for some well-known effects (gravitational lensing, Rees-Sciama, Sunyaev-Zel'dovich, Ostriker-Vishniac, second-order Sachs-Wolfe, Shapiro time-delay, inhomogeneous recombiation and reionization) as well as for a plethora of new terms, the latter being roughly equivalent to |fNL| ~ 1 or less (Nitta, Komatsu, Bartolo, Matarrese & Riotto 2009).

NG effects in LSS

Bartolo, Matarrese & Riotto (2005) computed the effects of NG in the dark matter density fluctuations in a matter-dominated universe. Only for high values of f_{NL} (~10) the standard parameterization is valid. For smaller primordial NG strength non-Newtonian gravitational terms shift f_{NL} by a term ~ 1 which depends on shape. On small scales stagnation effects during radiation dominance have to be taken into account up to second order (see Bartolo, Matarrese & Riotto 2007; Creminelli et al. 2008; Senatore et al. 2009).

Sefusatti & Komatsu (2007) show that LSS becomes competitive with CMB at $z > 2$; Jeong & Komatsu (2009) and Sefusatti (2009) compute one-loop bispectrum of bias objects.

NG and LSS

NG in LSS (to make contact with the CMB definition) can be defined through a potential Φ defined starting from the DM density fluctuation δ through Poisson's equation (use comoving gauge for density fluctuation, Bardeen 1980)

$$\delta = -\left(\frac{3}{2}\Omega_m H^2\right)^{-1} \nabla^2 \Phi$$

Many primordial (inflationary) models of non-Gaussianity can be represented in configuration space by the simple formula (Salopek & Bond 1990; Gangui et al. 1994; Verde et al. 1999; Komatsu & Spergel 2001)

$$\Phi = \phi_L + f_{NL}(\phi_L^2 - \langle \phi_L^2 \rangle) + g_{NL}\phi_L^3 + \ldots$$

Φ on sub-horizon scales reduces to minus the large-scale gravitational potential, ϕ_L its linear Gaussian contribution and f_{NL} is a dimensionless non-linearity parameter (or more generally non-linearity function). The percent of non-Gaussianity in CMB data implied by this model is NG % ~ 10^{-5} $|f_{NL}|$ which is < 10^{-3} - 10^{-4} (from present limits). For $|f_{NL}| >> 1$ this definition is indentical to the CMB (up to a normalization factor ~ 1.3 coming from DE driven evolution of the linear gravitational potential).

N-body simultions with Non-Gaussian initial data

$$\Phi = \Phi_L + f_{NL}(\Phi_L^2 - \langle \Phi_L^2 \rangle)$$

$$\nabla^2(\Phi * T)g(z) = -4\pi G a^2 \delta\rho_{DM}$$

growth suppression factor

matter transfer function

Grossi, Branchini, Dolag, Matarrese
& Moscardini 2007, …

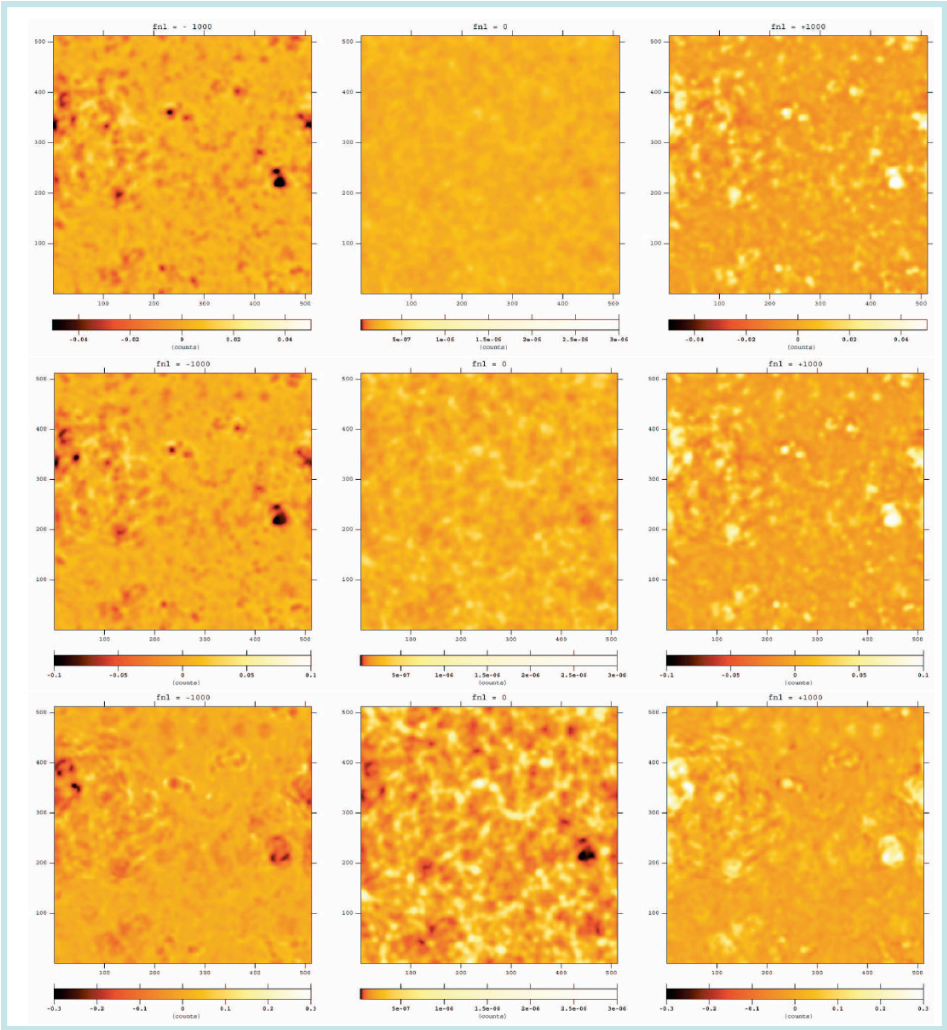

Figure 1. Slice maps of simulated mass density fields at $z = 5.15$ (*top*), $z = 2.13$ (*middle*) and $z = 0$ (*bottom*). The number of pixels at a side length is 512 ($500h^{-1}$Mpc) and that of the thickness is 32 ($31.25h^{-1}$Mpc). The panels in the middle row show the log of the projected density smoothed with a Gaussian filter of 10 pixels width, corresponding to $9.8h^{-1}$Mpc. The left and right panels are the relative residuals for the $f_{\rm NL}$=±1000 runs (equation [17]). Each panel has the corresponding color bar and the range considered are different from panel to panel.

DM halos in NG simulations

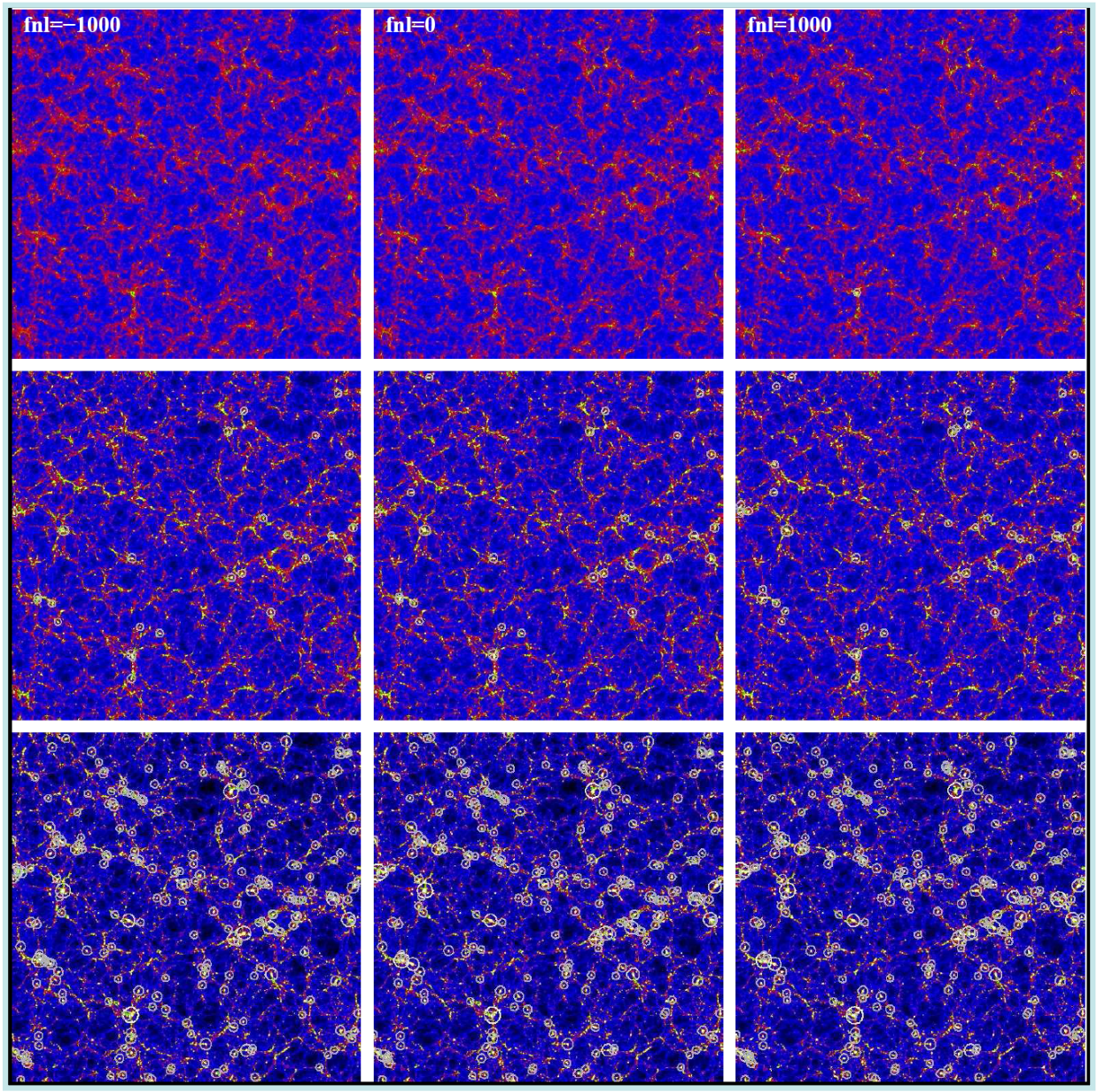

Grossi et al. 2008

Searching for non-Gaussianity with rare events

- Besides using standard statistical estimators, like bispectrum, trispectrum, three and four-point function, skewness , etc. …, one can look at the tails of the distribution, i.e. at rare events.

- Rare events have the advantage that they often maximize deviations from what predicted by a Gaussian distribution, but have the obvious disadvantage of being rare! But remember that, according to Press-Schechter-like schemes, all collapsed DM halos correspond to (rare) peaks of the underlying density field.

- Matarrese, Verde & Jimenez (2000) and Verde, Jimenez, Kamionkowski & Matarrese showed that clusters at high redshift (z>1) can probe NG down to $f_{NL} \sim 10^2$ which is, however, not competitive with future CMB (Planck) constraints.

- Alternative approach by LoVerde et al. (2007). Determination of mass function using stochastic approach (first-crossing probability of a diffusive barrier) Maggiore & Riotto 2009. Ellispsoidal collapse used by Lam & Sheth 2009.

- Excellent agreement of analytical formulae with N-body simulations found by Grossi et al. 2009

DM halo mass function vs fNL

Theoretical mass-function for NG fields:
Matarrese, Verde & Jimenez 2000;
LoVerde et al. 2008;
Maggiore & Riotto 2009;
Lam & Sheth 2009

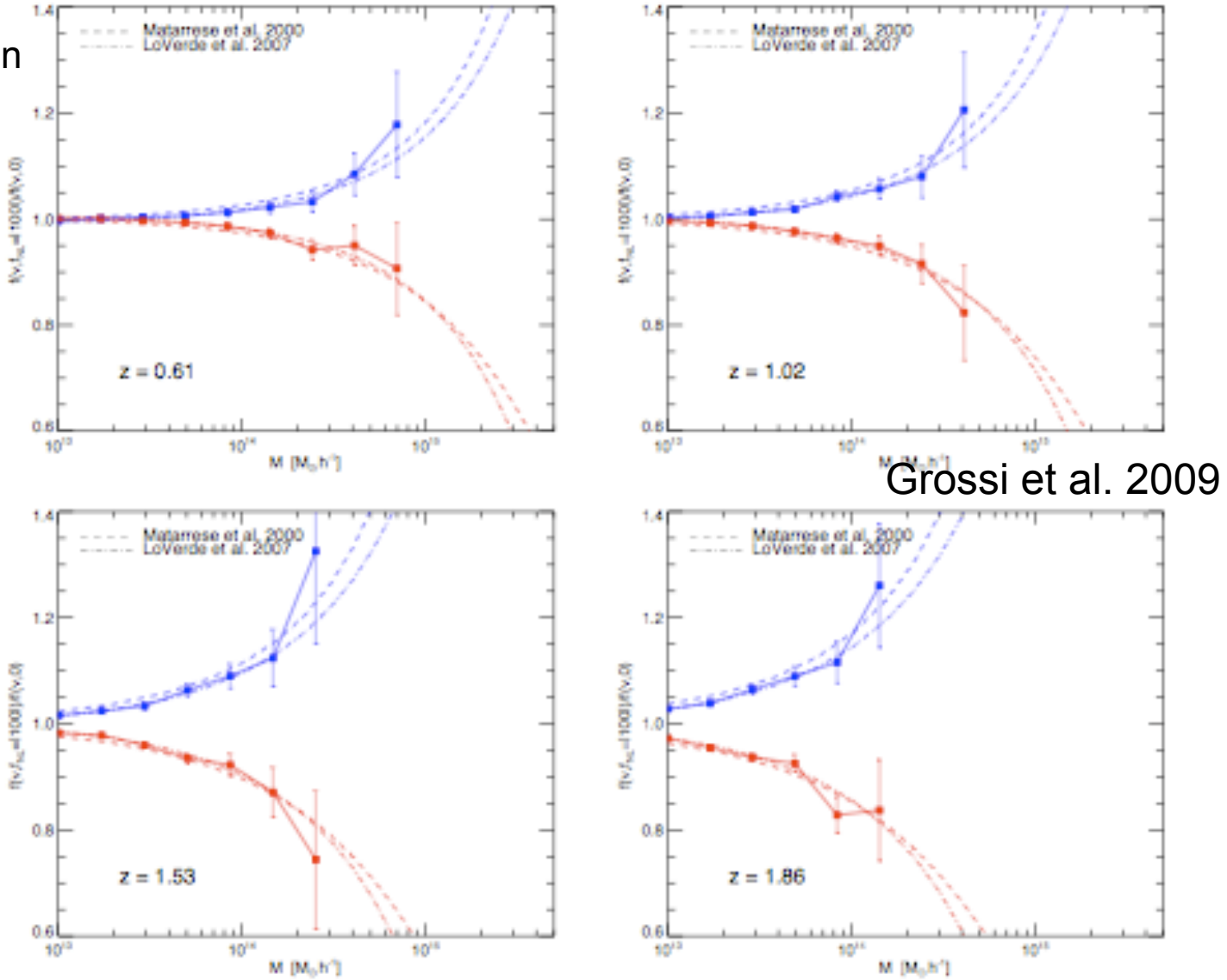

Grossi et al. 2009

Figure 6. Ratio of the non-Gaussian ($f_{NL} = \pm 100$) to Gaussian mass function for different redshift snapshots: top left $z = 0.61$; top right $z = 1.02$; bottom left $z = 1.53$; bottom right $z = 1.86$. The dashed line is the mass function of Matarrese, Verde & Jimenez (2001) and the dot-dashed lines are that of LoVerde et al. (2008), both including the q-correction.

DM halo clustering as a constraint on NG

$$\delta_{halo} = b\, \delta_{matter}$$

Dalal et al. (2007) have shown that halo bias is sensitive to primordial non-Gaussianity
through a scale-dependent correction term

$$\Delta b(k)/b \;\alpha\; 2\, f_{NL} \delta_c / k^2$$

This opens interesting prospects for constraining or measuring NG in LSS but demands for an accurate evaluation of the effects of (general) NG on halo biasing.

Dalal, Dore', Huterer & Shirokov 2007

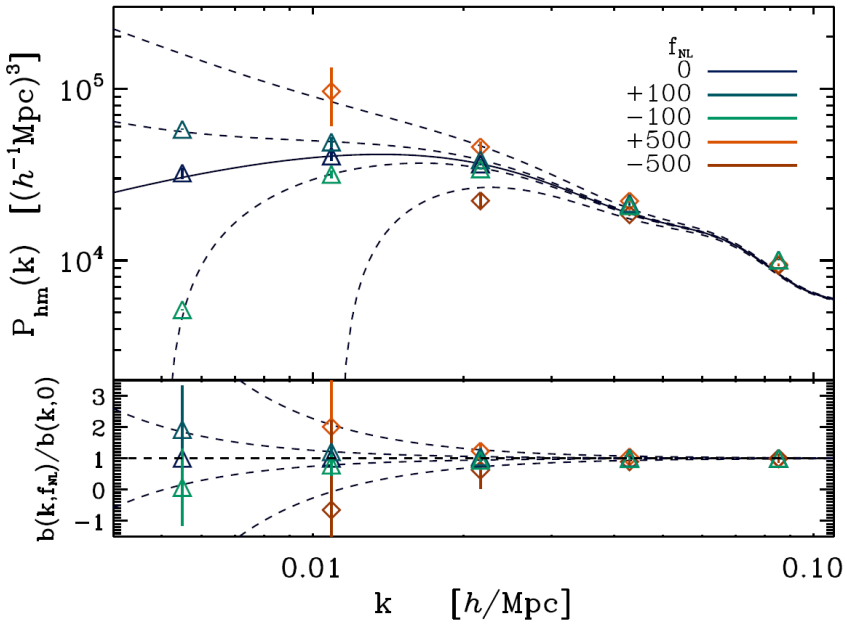

Clustering of peaks (DM halos) of NG density field

Start from results obtained in the 80's by

Grinstein & Wise 1986, ApJ, 310, 19

Matarrese, Lucchin & Bonometto 1986, ApJ, 310, L21

giving the general expression for the peak 2-point function as a function of N-point connected correlation functions of the background linear (i.e. Lagrangian) mass-density field

$$\xi_{h,M}(|\mathbf{x}_1 - \mathbf{x}_2|) = -1 + \exp\left\{ \sum_{N=2}^{\infty} \sum_{j=1}^{N-1} \frac{\nu^N \sigma_R^{-N}}{j!(N-1)!} \xi^{(N)} \begin{bmatrix} \mathbf{x}_1,\ldots,\mathbf{x}_1, & \mathbf{x}_2,\ldots\ldots,\mathbf{x}_2 \\ j\,times & (N-j)\,times \end{bmatrix} \right\}$$

(requires use of path-integral, cluster expansion, multinomial theorem and asymptotic expansion). The analysis of NG models was motivated by a paper by Vittorio, Juszkiewicz and Davis (1986) on bulk flows.

THE ASTROPHYSICAL JOURNAL, 310:L21–L26, 1986 November 1

A PATH-INTEGRAL APPROACH TO LARGE-SCALE MATTER DISTRIBUTION ORIGINATED BY NON-GAUSSIAN FLUCTUATIONS

SABINO MATARRESE
International School for Advanced Studies, Trieste, Italy
FRANCESCO LUCCHIN
Dipartimento di Fisica G. Galilei, Padova, Italy
AND
SILVIO A. BONOMETTO
International School for Advanced Studies, Trieste, Italy; Dipartimento di Fisica G. Galilei, Padova, Italy; and INFN, Sezione di Padova
Received 1986 July 7; accepted 1986 August 1

ABSTRACT

The possibility that, in the framework of a biased theory of galaxy clustering, the underlying matter distribution be non-Gaussian itself, because of the very mechanisms generating its present status, is explored. We show that a number of contradictory results, seemingly present in large-scale data, in principle can recover full coherence, once the requirement that the underlying matter distribution be Gaussian is dropped. For example, in the present framework the requirement that the two-point correlation functions vanish at the same scale (for different kinds of objects) is overcome. A general formula, showing the effects of a non-Gaussian background on the expression of three-point correlations in terms of two-point correlations, is given.

Subject heading: galaxies: clustering

THE ASTROPHYSICAL JOURNAL, 310:19–22, 1986 November 1

NON-GAUSSIAN FLUCTUATIONS AND THE CORRELATIONS OF GALAXIES OR RICH CLUSTERS OF GALAXIES[1]

BENJAMIN GRINSTEIN[2] AND MARK B. WISE[3]
California Institute of Technology
Received 1986 March 6; accepted 1986 April 18

ABSTRACT

Natural primordial mass density fluctuations are those for which the probability distribution, for mass density fluctuations averaged over the horizon volume, is independent of time. This criterion determines that the two-point correlation of mass density fluctuations has a Zeldovich power spectrum (i.e., a power spectrum proportional to k at small wavenumbers) but allows for many types of reduced (connected) higher correlations. Assuming galaxies or rich clusters of galaxies arise wherever suitably averaged natural mass density fluctuations are unusually large, we show that the two-point correlation of galaxies or rich clusters of galaxies can have significantly more power at small wavenumbers (e.g., a power spectrum proportional to $1/k$ at small wavenumbers) than the Zeldovich spectrum. This behavior is caused by the non-Gaussian part of the probability distribution for the primordial mass density fluctuations.

Subject headings: cosmology — galaxies: clustering

Peaks of NG random fields

- For a D-dimensional random field ε, filtered on scale R one defines a "peak operator"

$$n_{>\nu}(\mathbf{x},R) = \int_D d\omega (-1)^D \det\omega \;\; \Theta_H(\varepsilon_R(\mathbf{x}) - \nu\sigma_R)\delta^{(D)}(\partial_i\varepsilon_R(\mathbf{x}))\delta^{(D(D+1)/2)}(\partial_i\partial_j\varepsilon_R(\mathbf{x}) - \omega_{ij})$$

where one considers only peaks with heigth ilarger than ν times the rms fluctuation (on scale R). Here the domain D is over all negative definite symmetric matrices. For high threshold ν one expect one peak for every up-crossing region. In such a case one can compute the N-point function of $n_{>\nu}$ by standard QFT techniques (path-integral + cluster expansion) finding (Matarrese et al. 1986)

$$\Pi^{(N)}_{*,R}(x_1,\ldots,x_N) = \sum_{L=0}^{\infty}\sum_{\{m_L\}}\left[\prod_{s=1}^{L}\prod_{\{r_a\}=1}^{N}\left(w^{(s)}_{R,\{r_a\}}/s!\right)^{m_{s,\{r_a\}}}/m_{s,\{r_a\}}!\right]\prod_{r=1}^{N}a_{m_r}(2^{-1/2}\nu)$$

with

$$a_0(z) = (1/2)\,\mathrm{erfc}(z)$$
$$a_m(z) = \pi^{-1/2}2^{-m/2}\,e^{-z^2}H_{m-1}(z) \qquad (m>0)$$

and

$$w^{(2)}_{R,\{r_1 r_2\}} = \xi^{(2)}_R(x_{r_1},x_{r_2})/\sigma_R^2 \qquad (r_1\neq r_2)$$
$$w^{(2)}_{R,\{r_1 r_2\}} = 0 \qquad (r_1 = r_2)$$
$$w^{(n)}_{R,\{r_a\}} = \xi^{(n)}_R(x_{r_1},\ldots,x_{r_n})/\sigma_R^n \qquad (n>2)$$

Halo bias in NG models

- Matarrese & Verde 2008 have applied this relation to the case of local NG of the gravitational potential, obtaining the power-spectrum of dark matter halos modeled as high "peaks" (upcrossing regions) of height $\nu=\delta_c/\sigma_R$ of the underlying mass density field (Kaiser's model). Here $\delta_c(z)$ is the critical overdensity for collapse (at redshift a) and σ_R is the *rms* mass fluctuation on scale R ($M \sim R^3$)

- Next, account for motion of peaks (going from Lagrangian to Eulerian space), which implies (Catelan et al. 1998)

$$1+\delta_h(\mathbf{x}_{Eulerian})=(1+\delta_h(\mathbf{x}_{Lagrangian}))(1+\delta_R(\mathbf{x}_{Eulerian}))$$

  and (to linear order) $b=1+b_L$ (Mo & White 1996) to get the scale-dependent halo bias in the presence of NG initial conditions.

- Similar formulae apply to the correlation of CMB hot & cold spots (Heavens, Liguori, Matarrese, Tojeiro & Verde, in prep.)

- Alternative approach (based on 1-loop calculations by Taruya et al. (2008)

Halo bias in NG models

Matarrese & Verde 2008

$$b_{\rm h}^{f_{\rm NL}} = 1 + \frac{\Delta_c(z)}{\sigma_R^2 D^2(z)} \left[1 + 2 f_{\rm NL} \frac{\Delta_c(z)}{D(z)} \frac{\mathcal{F}_R(k)}{\mathcal{M}_R(k)} \right]$$

form factor:

$$\mathcal{F}_R(k) = \frac{1}{8\pi^2 \sigma_R^2} \int dk_1 k_1^2 \mathcal{M}_R(k_1) P_\phi(k_1) \times \int_{-1}^{1} d\mu \mathcal{M}_R\left(\sqrt{\alpha}\right) \left[\frac{P_\phi\left(\sqrt{\alpha}\right)}{P_\phi(k)} + 2 \right]$$

$$\alpha = k_1^2 + k^2 + 2 k_1 k \mu$$

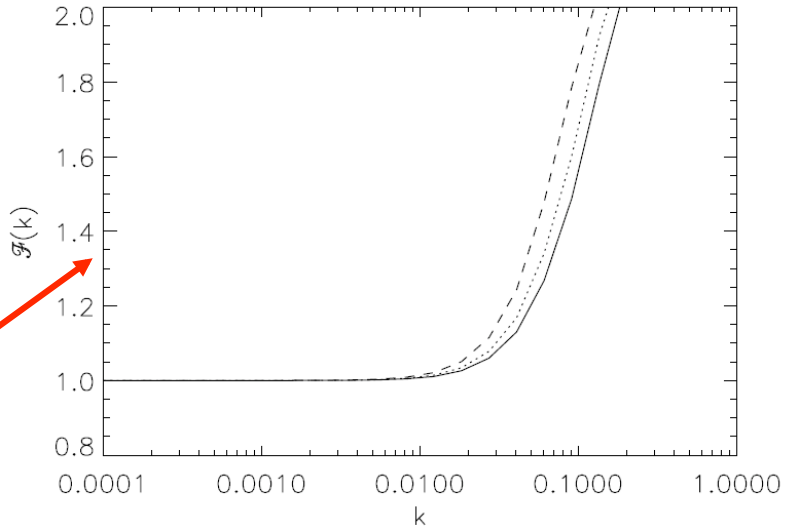

FIG. 1.— The function $\mathcal{F}_R(k)$ for three different masses: 1×10^{14} $M_\odot$ (solid), 2×10^{14} $M_\odot$ (dotted), 1×10^{15} $M_\odot$ (dashed).

factor connecting the smoothed linear overdensity with the primordial potential:

power-spectrum of a Gaussian gravitational potential

$$\mathcal{M}_R(k) = \frac{2}{3} \frac{T(k) k^2}{H_0^2 \Omega_{m,0}} W_R(k)$$

transfer function:

window function defining the radius R of a proto-halo of mass M(R):

Halo bias in NG models

- Extension to general (scale and configuration dependent) NG is straightforward

- In full generality write the ϕ bispectrum as $B_\phi(k_1,k_2,k_3)$. The relative NG correction to the halo bias is

$$\frac{\Delta b_h}{b_h} = \frac{\Delta_c(z)}{D(z)} \frac{1}{8\pi^2\sigma_R^2} \int dk_1 k_1^2 \mathcal{M}_R(k_1) \times$$
$$\int_{-1}^{1} d\mu \mathcal{M}_R\left(\sqrt{\alpha}\right) \frac{B_\phi(k_1,\sqrt{\alpha},k)}{P_\phi(k)} \times \frac{1}{M_R(k)}$$
$$\alpha = k_1^2 + k^2 + 2k_1 k\mu$$

- It also applies to non-local (e.g. “equilateral”) NG (DBI, ghost inflation, etc..) and universal NG term!!

Calibration on simulations

Grossi, Verde, Dolag, Branchini, Carbone, Iannuzzi, Matarrese & Moscardini 2009

Local non-Gaussianity

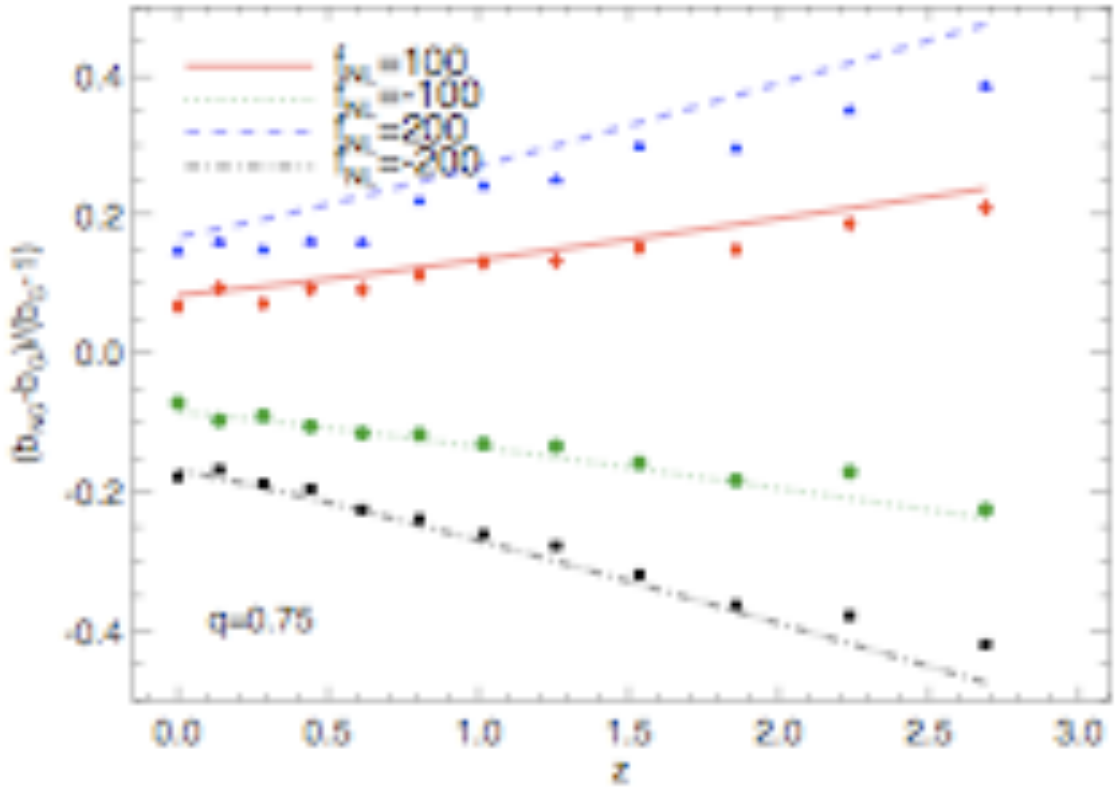

Figure 12. The redshift dependence of the non-Gaussian correction to the halo bias: points are the values measured from the simulations, lines are the theoretical predictions, Eq. (9). Only $k < 0.026\ h/Mpc$ were used.

Observational prospects

On these large scales only the “two halo” term counts

Fisher matrix approach (Carbone, Verde & Matarrese 08):

From the P(k) shape

survey	z range	sq deg	mean galaxy density $(h/Mpc)^3$	$\Delta f_{\rm NL}/q'$ LSS
SDSS LRG's	$0.16 < z < 0.47$	7.6×10^3	1.36×10^{-4}	40
BOSS	$0 < z < 0.7$	10^4	2.66×10^{-4}	18
WFMOS low z	$0.5 < z < 1.3$	2×10^3	4.88×10^{-4}	15
WFMOS high z	$2.3 < z < 3.3$	3×10^2	4.55×10^{-4}	17
ADEPT	$1 < z < 2$	2.8×10^4	9.37×10^{-4}	→ 1.5
EUCLID	$0 < z < 2$	2×10^4	1.56×10^{-3}	→ 1.7
DES	$0.2 < z < 1.3$	5×10^3	1.85×10^{-3}	8
PanSTARRS	$0 < z < 1.2$	3×10^4	1.72×10^{-3}	3.5
LSST	$0.3 < z < 3.6$	3×10^4	2.77×10^{-3}	→ 0.7

ISW is found to be less powerful. See Afshordi & Tolley 08 for S/N

Observational status

Data/method	$f_{\rm NL}$	reference
Photometric LRG - bias	$63^{+54+101}_{-85-331}$	Slosar et al. 2008
Spectroscopic LRG- bias	$70^{+74+139}_{-83-191}$	Slosar et al. 2008
QSO - bias	8^{+26+47}_{-37-77}	Slosar et al. 2008
combined	28^{+23+42}_{-24-57}	Slosar et al. 2008
NVSS–ISW	$105^{+647+755}_{-337-1157}$	Slosar et al. 2008
NVSS–ISW	$236 \pm 127(2-\sigma)$	Afshordi&Tolley 2008
WMAP3-Bispectrum	30 ± 84	Spergel et al. (WAMP) 2007
WMAP3-Bispectrum	32 ± 68	Creminelli et al 2007
WMAP3-Bispectrum	87 ± 60	Yadav & Wandelt 2008
WMAP5-Bispectrum	51 ± 60	Komatsu et al. (WMAP) 2008
WMAP5-Minkowski	-57 ± 121	Komatsu et al. (WMAP) 2008

Local-type only, 2 σ errors

Observational prospects

Data/method	$\Delta f_{\rm NL}\ (1-\sigma)$	reference
BOSS–bias	18	Carbone et al 2008
ADEPT/Euclid–bias	1.5	Carbone et al 2008
PANNStarrs –bias	3.5	Carbone et al 2008
LSST–bias	0.7	Carbone et al 2008
LSST-ISW	7	Afshordi& Tolley 2008
BOSS–bispectrum	35	Sefusatti & Komatsu 2008
ADEPT/Euclid –bispectrum	3.6	Sefusatti & Komatsu 2008
Planck-Bispectrum	3	Yadav et al . 2007
BPOL-Bispectrum	2	Yadav et al . 2007

The bispectrum sees the “shape”, halo bias does not!

Effect of universal NG from PN terms

Verde, Carbone & Matarrese
In prep.

Effect equivalent to f_{NL} ~ few

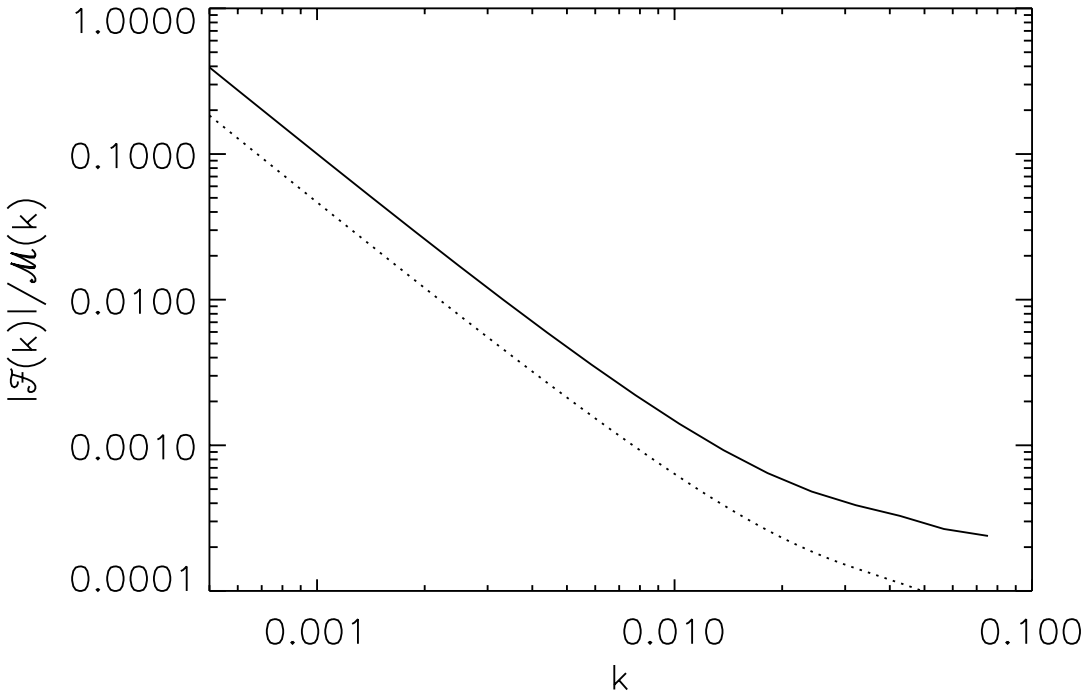

Can we detect inflationary NG via the 21-cm background?

Pillepich, Porciani & Matarrese, 2006

see also Cooray 2006; Cooray et al. 2008

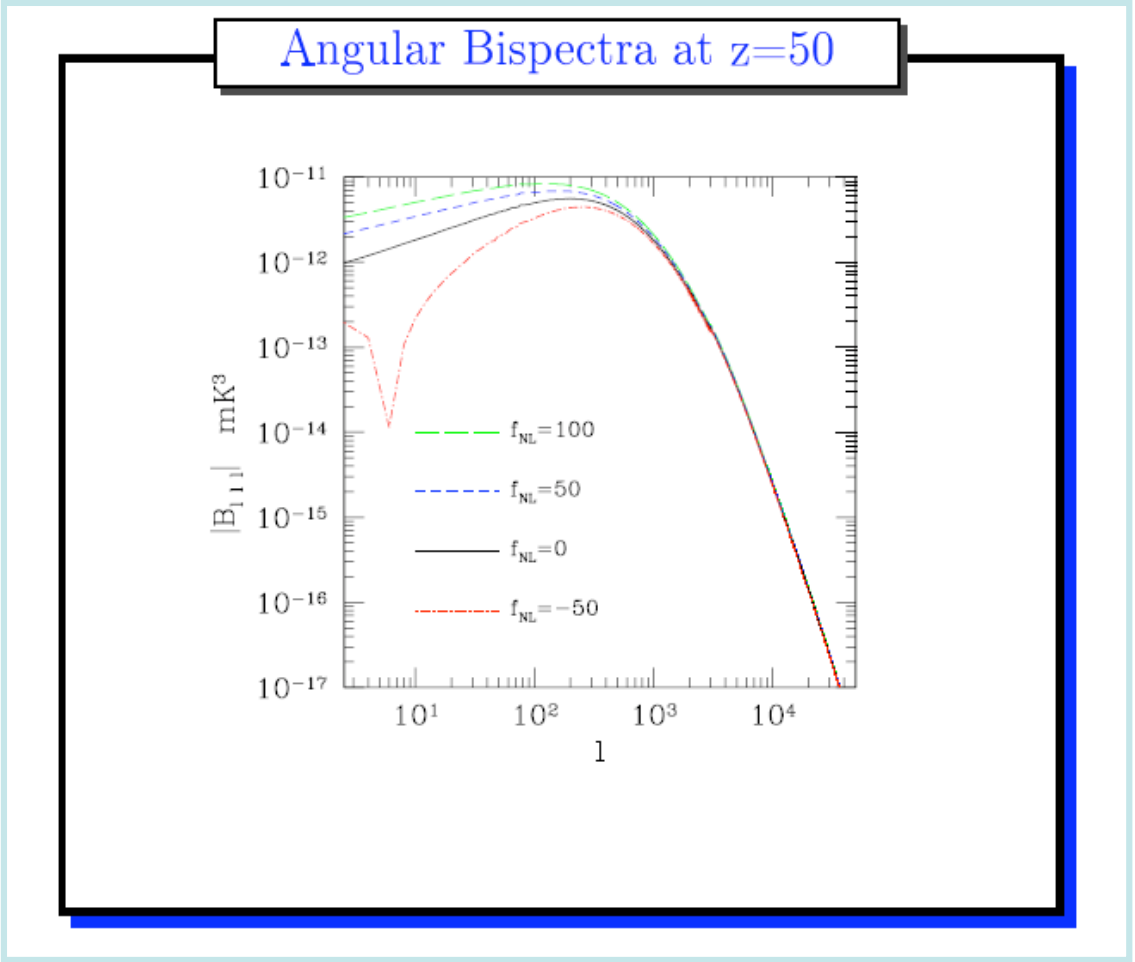

Is the expected NG signal detectable by future radio experiments?

Pillepich, Porciani & Matarrese 2006
Cooray 2006, Cooray et al. 2007

Hypotheses:

- Ideal, full-sky experiment
- Measurements limited by cosmic variance only
- Perfect subtraction of foregrounds

Warning: gravitational lensing can be very important!

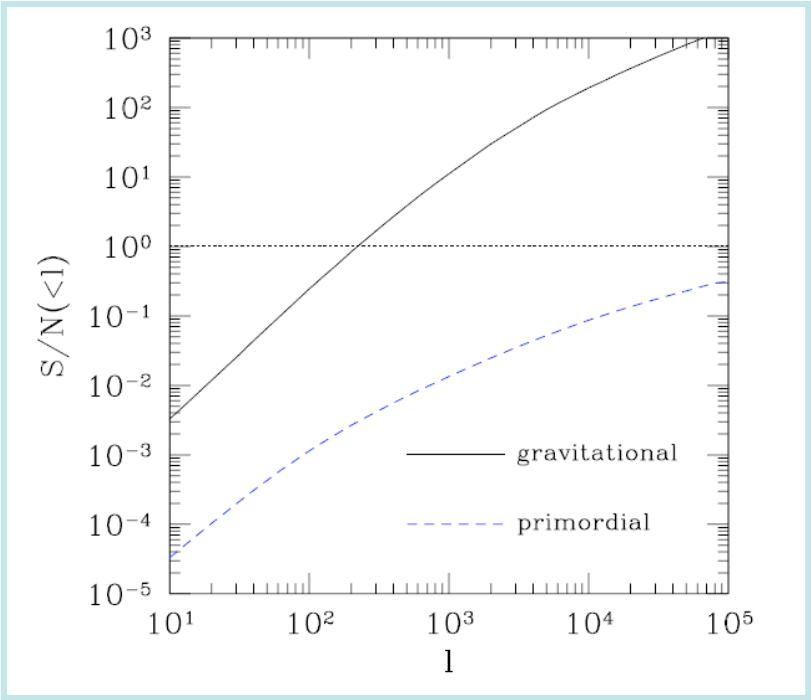

Experiments with arcmin-scale resolution can measure →

- gravitational NG with S/N ~ 100
- primordial NG with S/N ~ 0.1 f_{NL}

Non-Gaussianities in the IGM

Viel, Dolag, Branchini, Grossi, Matarrese & Moscardini 2008

Very first NG hydro simulations

NG initial conditions:

$$\Phi = \Phi_L + f_{NL}(\Phi_L^2 - \langle \Phi_L^2 \rangle)$$

$$\nabla^2(\Phi * T)g(z) = -4\pi G a^2 \delta\rho_{DM}$$

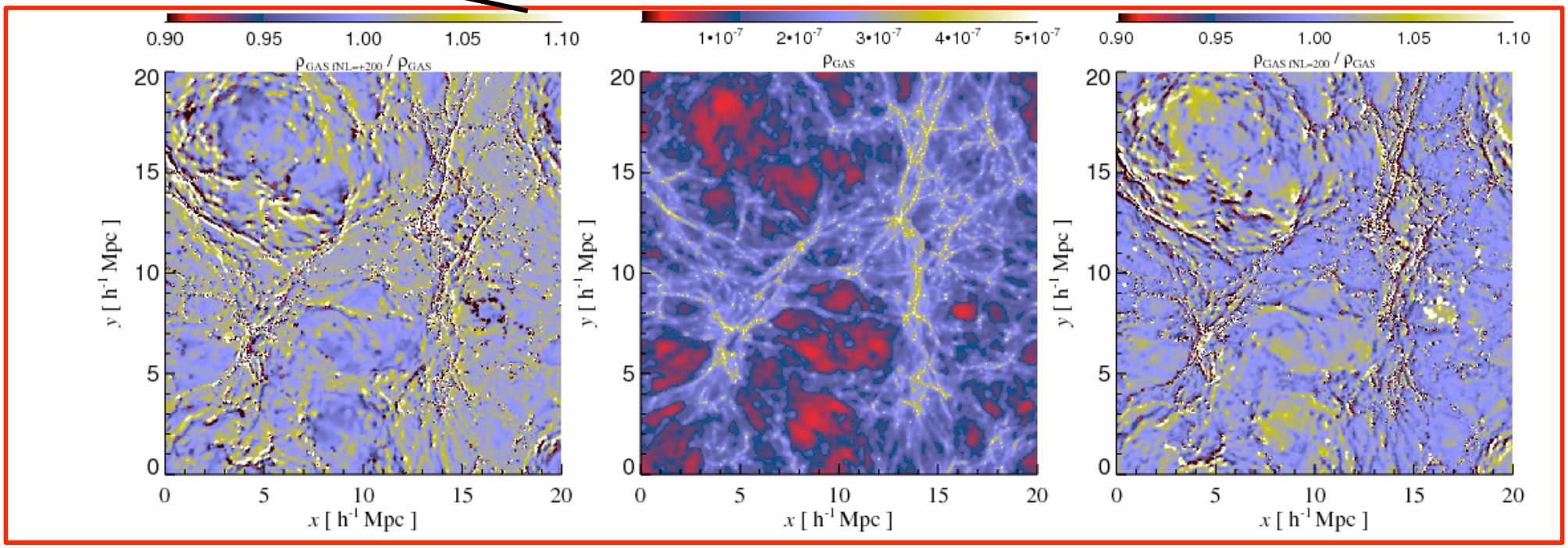

NG/G f_{NL} = 100 f_{NL} = 0 f_{NL} = - 100

GAS distribution in a slice of 3 Mpc/h (comoving) at z=3 (the voids have less and more matter compared to the standard case) – this in turn can be seen in the flux PDF

Need to go beyond standard perturbation theory

- (Linear) perturbation theory proved extremely successful in dealing with CMB data
- The study of the LSS requires better schemes, owing to the crucial role played by the gravitational instability, which makes the underlying dark matter density field unavoidably non-linear, hence non-Gaussian, on a relevant range of scales.
- Renormalized Perturbation Theory (Crocce & Scoccimarro 2005, 2006)
- Renormalization Group (RG) approach (Matarrese & Pietroni 2007; Pietroni 2008)

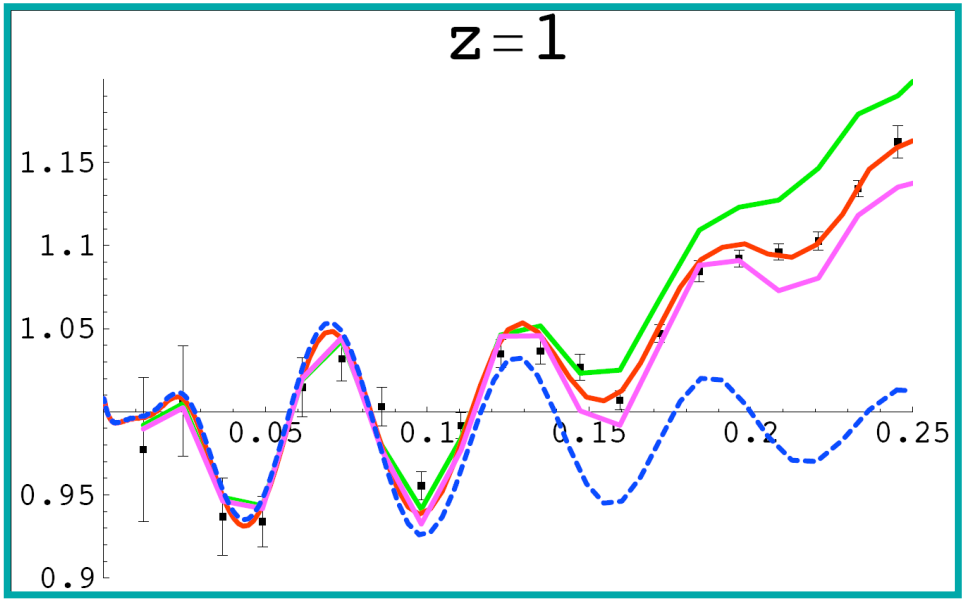

Power-spectrum at z=1as given by RG (red line), linear theory (blue short-dashed), 1-loop PT (green), halo-model (violet) and N-body simulations (squares) by Jeong & Komatsu 2006

Comparison with N-body data

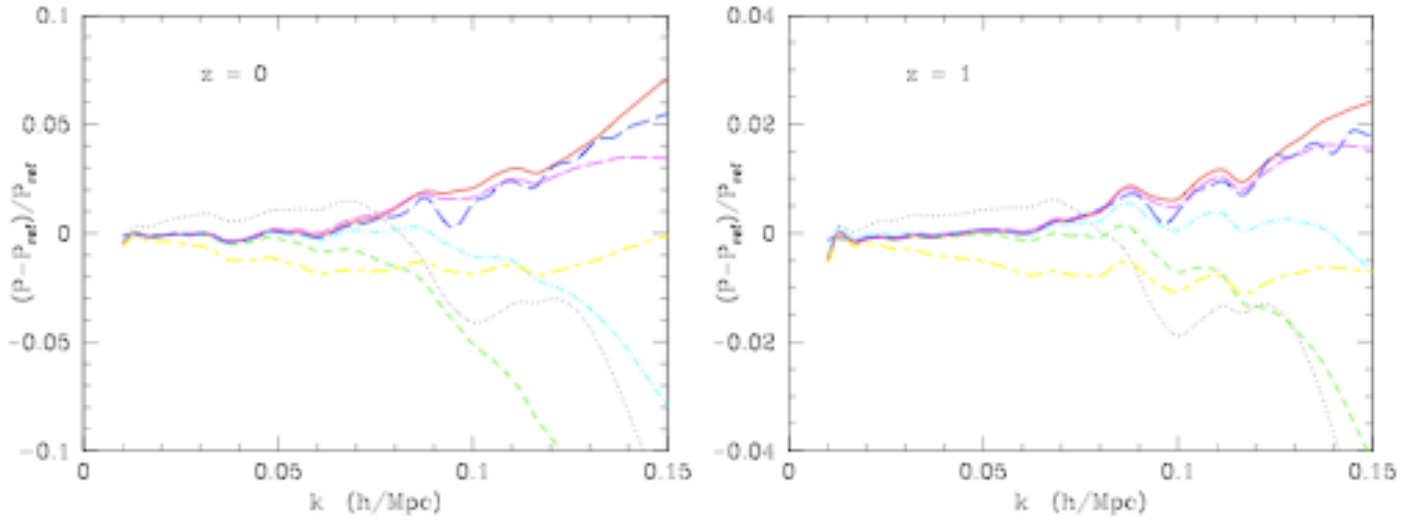

FIG. 5: The fractional deviation of each method from the reference spectrum, for ΛCDM at $z = 0$ (left) and $z = 1$ (right). This figure focuses on the region $k < 0.15\,h\,\mathrm{Mpc}^{-1}$ where linear theory is inadequate but higher order methods are still viable. As in Figure 4 the (black) dotted line is linear theory, the (red) solid line is 2-loop SPT, the (blue) long-dashed line is 2-loop RPT, the (green) short-dashed line is Lagrangian resummation, the thick (cyan) dot-short dashed line is 2-loop closure theory the thick (magenta) dot-long dashed line is the large-N expansion, and the thick (yellow) short-long dashed line is time-RG theory.

Carlson, White & Padmanabhan 2009

RG: short & long-term goals

- Include neutrino contribution (Lesgourgues, Matarrese, Pietroni & Riotto, 2009)
- Account for (*statistical*) velocity dispersion, starting from the Vlasov equation (D'Amico, Matarrese & Pietroni in prep.). Explains damping of small-scale modes
- Deal with redshift-space distortions and non-linear mass → galaxy bias
- Extend the method to higher-order: non-linear evaluation of the bispectrum

Conclusions

- Prospects for probing inflation via gravitational-wave detection via CMB polarization are in good shape. But primordial gravitational waves appear to be detectable only if the inflation energy scale is larger than ~ 10^{15} GeV.

- Contrary to earlier naive expectations, some level of non-Gaussianity is generically present in *all inflation models*. The level of non-Gaussianity predicted in the simplest (single-field, slow-roll) inflation is slightly below the minimum value detectable by *Planck* and at reach of future galaxy surveys.

- Constraining/detecting non-Gaussianity is a powerful tool to discriminate among competing scenarios for perturbation generation (*standard slow-roll inflation, curvaton, modulated-reheating, DBI, ghost inflation, multi-field, etc. …*) some of which imply large non-Gaussianity. Non-Gaussianity will soon become the *smoking-gun* for non-standard inflation models

- The *Planck* mission (in combination with future galaxy surveys) will open a new window to the physics of the early Universe.